Neuronal Activity Represses Oncologic Transformation of Cerebellar External Granule Cells in Medulloblastoma

Claire L. Chabot

Department of Human Genetics

Faculty of Medicine and Health Sciences

McGill University, Montreal

March 2022

A thesis submitted to McGill University in partial fulfillment of the requirements of the degree of Master of Science in the faculty of Department of Medicine, Human Genetics

Abstract

Medulloblastoma (MB) is the most prevalent, metastatic pediatric brain tumor and has the highest mortality rate for childhood cancers. In Canada alone, the 25 – 50 children that are diagnosed with MB annually account for 15-25% of all pediatric brain tumours. This research focuses on the SHH MB subgroup which is prevalent in 30% of MB tumors. The cells of origin for SHH MB are cerebellar granule neuron precursors (cGNPs) in the external granule cell layer (EGL) on the surface of the cerebellum. During brain development, cGNPs migrate tangentially and actively proliferate in response to SHH, then migrate radially towards the internal granule cell layer (IGL) to differentiate. Our lab's previous work demonstrated that a glutamate gradient, originating from the differentiated cells of the IGL may be diffusing towards undifferentiated cGNPs to initiate membrane depolarization, cell cycle exit, and differentiation. We hypothesized that neural activity impairs oncogenic transformation of cerebral granule neuron precursors and is tumor suppressive in SHH MB. We began by characterising the effects of neurotransmitters such as Glutamate and Gaba on cGNPs from P7 mice. The addition of Glutamate and GABA to cGNP cultures demonstrated an anti-proliferative effect despite the presence of a Shh agonist (SAG). Following this, glutamate production in P7 cerebellar cultures in vitro was measured to delineate the effect of glutamate on differential neural activity at different times of postnatal mouse cerebellum development. The results displayed a significant increase in glutamate production by P15 and P21 while simultaneously displaying glutamate's presence in the post-natal brain as early as P5. Lastly, we measured spontaneous neural activity during development using RNA *in-situ* hybridization with c-fos and math1/atoh1 probes to understand whether that the *in vivo* glutamate gradient translates into increased neural activity. Early expression of the c-fos marker in undifferentiated cells demonstrated the presence of depolarising events in the EGL before synapses are formed in the IGL. Co-expression of math1 and c-fos in the int-EGL

indicates the expression and manifestation of neural activity is an early event in differentiation in granule cells and the quantification of fluorescence using ImageJ compounded these results. Results from this thesis indicate that a glutamate gradient drives spontaneous neural activity in the cerebellum to counterbalance Shh induced proliferation and drive cell-cycle exit and differentiation.

Résumé

Le médulloblastome (MB) est la tumeur cérébrale pédiatrique métastatique la plus répandue et présente le taux de mortalité le plus élevé pour les cancers infantiles. Au Canada seulement, les 25 à 50 enfants qui reçoivent un diagnostic de MB chaque année représentent de 15 à 25 % de toutes les tumeurs cérébrales chez les enfants. Cette recherche se concentre sur le sous-groupe SHH MB qui est répandu dans 30% des tumeurs MB. Les cellules d'origine de SHH MB sont des précurseurs de neurones de granules cérébelleux (cGNPs) dans la couche externe de cellules de granule (EGL) à la surface du cervelet. Pendant le développement du cerveau, les cGNPs migrent tangentiellement et activement prolifèrent en réponse à SHH, puis migrent radialement vers la couche de granules cellulaires internes (IGL) pour se différencier. Les travaux antérieurs de notre laboratoire ont démontré qu'un gradient de glutamate, provenant des cellules différenciées de l'IGL peut se diffuser vers des cGNPs indifférenciés pour initier la dépolarisation membranaire, la sortie du cycle cellulaire et la différenciation. Nous avons émis l'hypothèse que l'activité neurale affecte la transformation oncogène des précurseurs neuronaux de granules cérébraux et est suppresseur de tumeur dans SHH MB. Nous avons commencé par caractériser les effets des neurotransmetteurs tels que Glutamate et Gaba sur les cGNPs de souris P7. L'ajout de glutamate et de GABA aux cultures cGNP a démontré un effet antiprolifératif malgré la présence d'un agoniste de Shh (SAG). Par la suite, la production de glutamate dans les cultures cérébelleuses P7 in vitro a été mesurée pour définir l'effet du glutamate sur l'activité neurale différentielle à différents moments du développement du cervelet postnatal chez la souris. Les résultats ont montré une augmentation significative de la production de glutamate par P15 et P21 tout en affichant simultanément la présence de glutamate dans le cerveau post-natal dès P5. Enfin, nous avons mesuré l'activité neuronale spontanée pendant le développement à l'aide de l'hybridation in situ de l'ARN avec des sondes c-fos et

math1/atoh1 pour comprendre si le gradient de glutamate in vivo se traduit par une activité neurale accrue. L'expression précoce du marqueur c-fos dans les cellules indifférenciées a démontré la présence d'événements dépolarisants dans l'EGL avant la formation de synapses dans l'IGL. La co-expression de math1 et c-fos dans l'int-EGL indique que l'expression et la manifestation de l'activité neurale est un événement précoce dans la différenciation des cellules granuleuses et la quantification de la fluorescence à l'aide d'ImageJ a composé ces résultats. Les résultats de cette thèse indiquent qu'un gradient de glutamate entraîne une activité neuronale spontanée dans le cervelet pour contrebalancer la prolifération induite par Shh et entraîner la sortie et la différenciation du cycle cellulaire.

Table of Contents

List of Abbreviations

AMPA	α-amino-3-hydroxy-5-methyl-4-isoxazolepropionic acid
APC	Anaphase-promoting complex
BCC	Basal cell carcinoma
BDNF	Brain-derived Neurotrophic Factor
bHLH	Basic helix loop-helix
BMP	Bone morphogenic protein
cGNP	Cerebellar granule neuron precursor
CK1	Casein Kinase 1
CNS	Central nervous system
CSF	Cranial spinal fluid
DEG	Differentiatlly expressed genes
DHH	Dessert hedgehog
DIV3	Cell division 3
DZ	Dorsomedial ventricular zone
EC50	Effective concentration 50%
EdU	5-ethynyl-2'-deoxyuridine
EGL	External granule layer
ext-EGL	External EGL
GABA	y-amino butyric acid
hChR2	Channelrhodopsin-2
HCL	Hydrochloric acid
HGG	High-grade glioma
HH	Hedgehog
IGL	Internal granule layer

IHH	Indian hedgehog
int-EGL	Internal EGL
IntDen	Integrated density
IsO	Isthmic organizer
LCA	Large cell anaplasia
LMD	Leptomeningeal dissemination
MB	Medulloblastoma
ML	Molecular layer
NMDA	N-methyl-D-aspartate
NT	Neurotransmitter
OPC	Oligodendrocyte precursor cell
PBS	Phosphate-Buffered Saline
PC	Primary cilium
PCL	Purkinje cell layer
PFA	Paraformaldehyde
RT-PCR	Reverse transcriptase polymerase chain reaction
SAG	Sonic hedgehog agonist
Shh	Sonic hedgehog
Smo	Smoothened protein
SNV	Single nucleotide variant
VGCC	Voltage gated calcium channel
VZ	Ventricular zone
WHO	World Health Organisation
WNT	Wingless

List of Figures and Tables

Figures

Acknowledgements

I would like to extend my sincerest gratitude to my supervisor, Dr. Livia Garzia. The door to Dr. Garzia's office was always open whenever I ran into a trouble spot or had a question about my research or writing. She consistently allowed this work to be my own work but steered me in the right direction whenever she believed I needed it and pushed me to do my best. Amongst other things, she has helped me develop my critical thinking skills and thank you, Dr. Garzia, for being patient and positive in the most trying of situations.

I would like to acknowledge all my committee members; Dr. Frederic Charron and Dr. Nada Jabado. I thank them for their time and valuable comments in my committee meeting sessions and during my project.

I want to acknowledge the support and love of my family through the process of completing this thesis. With each passing day, I learn more from each of you.

I extend a thank to Bryn Livingston, a BSc. Neuroscience student at McGill University who I helped supervise during my MSc. and who contributed to the progress of my thesis.

I would like to thank the animal facility members at the RI-MUHC for their patience and support in training me to handle mice and use them in my project. Also thank you, Core Facility, for helping me to prepare and cut my brain tissue for my in-situ experiments as well as the staff at the RI-MUHC Molecular Imaging Platform who aided me with my many hours at the confocal microscope.

Contribution of Authors

The work described in this thesis was performed under the supervision of Dr. Livia Garzia. It is a manuscript-based thesis format as described in the Thesis Preparation Guidelines by the Department of Graduate and Postdoctoral Studies of McGill University. This thesis was written entirely by myself (Claire L. Chabot). The work described herein is the research efforts for my graduate degree and was performed by me unless otherwise stated. I would like to recognise the work of previous lab member Bryn Livingston, an undergraduate student I supervised from 2019 – 2020, whose work contributed to the experiments I conducted during that time.

Chapter 1: Introduction

1. Medulloblastoma & Impact of Disease

1.1. Clinical Overview

Medulloblastoma (MB) is the most common malignant, paediatric brain tumour. Considered a fast growing (grade IV) tumour, MB spreads rapidly through cerebrospinal pathways and can form tumours along the ventricles of the CNS. The most aggressive forms of medulloblastoma occur in infants and young children (Kuzan-Fischer, Juraschka, & Taylor, 2018). It is also responsible for the most deaths in infants, children, and adolescents afflicted by cancer (Kuzan-Fischer et al., 2018; Levisohn, Cronin-Golomb, & Schmahmann, 2000). MB originates in the cerebellum which resides in the anterior end of the hindbrain (Fig.1) (Buckner, 2013). The cerebellum's main roles are mostly, but not entirely limited to, sensory-motor processing, balance control and movement regulation (Jimsheleishvili & Dididze, 2020). Patient prognosis is mostly dependent on the speed of replication, tumour location, and individual patient responses to treatment. Early onset symptoms of medulloblastoma are classified as, but not limited to, headaches, morning vomiting, issues retaining spatial memory, and complications controlling motor-skills and coordination (Cavalli et al., 2017; A. J. Gajjar & Robinson, 2014; Kuzan-Fischer et al., 2018). The current WHO histopathological classification for medulloblastoma divides MB into 5 subcategories: the classic subgroup (with only a few differentiated neurons), the desmoplastic variant (where tumour cells display some differentiation and are surrounded by an extracellular matrix), tumours with nodularity, and, lastly, anaplastic and large cell anaplastic tumours (both being the most aggressive and fatal forms of MB histopathology) (Louis et al., 2016). About 20-30% of MB cases presents with metastasis. Leptomeningeal dissemination (LMD) is also the leading cause of death (40%) for MB cases (Fults, Taylor, & Garzia, 2019).

Previously, it was postulated that MB metastasized exclusively throughout the central nervous system (CNS) hinting at the cranial spinal fluid (CSF) being the disseminated cells primary mode of transport (Fults et al., 2019). However, metastatic MB tumours can also spread to the bones, lungs, liver, and lymph nodes (Van Ommeren, Garzia, Holgado, Ramaswamy, & Taylor, 2020).

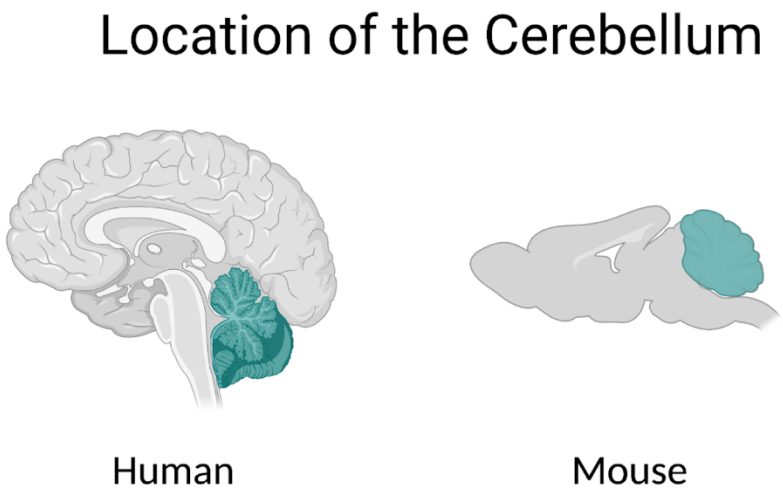

Fig. 1 | Anatomical location of the mammalian cerebellum Diagram representing the different anatomical locations of the adult cerebellum in both humans and mice. Created with BioRender.

1.2. Prevalence

In Canada alone, 25 – 50 children are diagnosed with medulloblastoma annually. Worldwide, approximately 0.74 per 100 000 children are at risk of developing MB every year (Roussel & Hatten, 2011). The majority of the medulloblastoma patient population (67%) consists of children ages 4-16 years of age (Kool et al., 2012). Infants (<4 years old) are the second-most frequently diagnosed group (21%), the rest of the patient population consisting of adults (16< years old) (Kool et al., 2012). Overall, the median age upon diagnosis is approximately 7.2 years old and, on average, outcomes for these patients are not very promising, even for survivors (Fogarty, Emmenegger, Grasfeder, Oliver, & Wechsler-Reya, 2007; Kool et al., 2012).

1.3. Treatment

Treatment for medulloblastoma begins with the patients undergoing surgical resection of the brain tumor followed by several rounds of craniospinal irradiation and chemotherapy (Kuzan-Fischer et al., 2018). Advances in contemporary treatment methods for medulloblastoma have led to a dramatic increase in 5-year survival rates for patients with average risk MB, in first-world countries, to approximately 60-70% (A. Gajjar et al., 2006; Kuzan-Fischer et al., 2018). For those diagnosed with high-risk medulloblastoma, 30% of them will die as a direct cause of their disease (Finlay, Erdreich-Epstein, & Packer, 2007). As the age upon diagnosis for MB tends to be very young, the harsh combination of chemotherapeutics and radiation to the developing brain can prove to be quite damaging with a list of adverse secondary effects (such as loss of hearing) which directly affect the patient's quality of life (A. Gajjar et al., 2006). Survivors tend to struggle to thrive in social and academic settings due to the long-term cognitive deficits inflicted by modern treatment protocols (Barrera, Shaw, Speechley, Maunsell, & Pogany, 2005; Moxon-Emre et al., 2014). Secondary-effects such as these arise due to the post-treatmnet neurcognitive impairment and endocrine deficiences. Secondary tumours, caused by the radiation treatment, potentially pose a threat to the patient's long-term survvial, and overall quality of life, and must be treated accordingly (Kuzan-Fischer et al., 2018). As we refine our understanding of the disease at the molecular level, we will no doubt improve diagnostic tools and develop new and improved targeted therapies.

1.4. Clinical Subgroups

In current literature, there are four known MB subgroups: wingless (WNT), sonic hedgehog (SHH), Group 3 and Group 4 (Taylor et al., 2012). What sets the subgroups apart from one another are their distinct genetic profiles, epidemiology, and patient outcomes (Cavalli et al., 2017; Northcott et al., 2012; Taylor et al., 2012). For a few of these subgroups, specifically

WNT and SHH MB, previous research has discerned their cells of origin allowing for further molecular characterise of MB tumorigenesis. The subgroups have also been more minutely categorized with heterogenous subtypes that can act as further prognostic markers for patients and their responsiveness to different treatment protocols (Holgado, Guerreiro Stucklin, Garzia, Daniels, & Taylor, 2017). In 2015, a new risk stratification protocol was designed in order to correlate variations in MB patient outcomes based on tumour subgroup classification (Ramaswamy et al., 2016). The four associated risk categories outlined in this protocol are "low risk" (>90% survival), "standard risk" (75-90% survival), "high risk" (50-75% survival), "very high risk" (< 50% survival). There are, however, a select few independent prognostic factors that, regardless of MB subgroup, have prominent effects on patient outcomes. One such determiner is the presence of mutations on MYC(N) which will be discussed in a later section of this thesis (Kool et al., 2012).

1.4.1. WNT Medulloblastoma

WNT MB is the least occurring of all the subgroups caping around a 10% occurrence in all patient diagnoses (Kool et al., 2012). This tumour classification is also practically absent in the infant age-group category (1% prevalence) whereas the age distribution for patients is generally between 10-12 years old (Kool et al., 2012; Luzzi et al., 2020). The cell of origin for WNT MB are progenitor cells located in the dorsal brain stem of the CNS (Kool et al., 2012). The importance of progenitors with WNT MB also strongly correlates to the namesake of this subgroup; the WNT pathway plays an important roles in cell fate determination, cell migration, cell polarity, neural patterning, and organogenesis during embryonic development of which progenitor cells are deeply involved in (Komiya & Habas, 2008). The primary driver mutations for WNT MB occur on CTNNB1 (90%), DDX3X (50%), SMARCA4 (25%), and TP53 (12.5%) (Luzzi et al., 2020). The protein beta-catenin plays an essential role

for both the canonical and noncanonical WNT pathway activation (Komiya & Habas, 2008). Therefore, when somatic mutations occur on CTNNB1, the gene necessary to produce beta-catenin, the nuclear localization of the beta-catenin protein leads to overactivation of the WNT pathway and becomes a main driver for the associated MB subgroup (Northcott et al., 2012). This mutation, compounded with mutations on TP53, generate the characteristic overactivation of the WNT pathway associated with this subgroup (Northcott et al., 2012). Since WTN tumour are arely, if at all, metastatic (5-10%), they are classified as "low-risk" under the 2015 risk-stratificiation protocol (Kuzan-Fischer et al., 2018; Luzzi et al., 2020). This prognosis is also reflected in the higher survival outcomes that WNT MB patients experience (> 90% 5-year survival) compared to their peers (Luzzi et al., 2020).

1.4.2. Group 3 & 4 Medulloblastoma

In current literature, Group 3 and Group 4 MB are the most poorly defined of the four subgroups. Both subgroups have a higher prevalence in males to females (2:1 and 3:1, respectfully) yet this correlation has no known effect on patient outcomes. The former makes up 25% of all MB cases while the latter, Group 4, is the most pervasive subgroup (35%) yet very poorly defined (Kool et al., 2012). Group 3 MB generally occurs in infants (<3 years old) and Group 4 is mostly observed in children (Luzzi et al., 2020). Cases associated with Group 3 have quanitfiably lower 5-year survival rates (40-60%), which is strongly correlated with the high prevalence of leptomeningeal dissemination (LMD) and metastaiss (45%) (Luzzi et al., 2020). This qualifies Group 3 MB for a "high-risk" classification on the MB risk assessment scale (Kuzan-Fischer et al., 2018). Oftentimes, Group 4 tumours become metastatic (30-40%) and share similar mutations to Group 3 tumours (such as GFI1/GFI1B) yet Group 4 is assigned to the "low-risk" category with favourable 5-year survival outcomes (75%) (Luzzi et al., 2020; Pietsch et al., 2014; Ramaswamy et al., 2016). Future

experimentation must be run to understand the molecular roots of these pervasive MB subgropus in order to provide better personalized care for patients.

1.4.3. SHH Medulloblastoma

The fourth subgroup, as well as the focus of this thesis, is SHH MB. The cell of origin SHH tumours are cerebellar granule neuron precursors (cGNPs), and tumours arise either in the cerebellar hemispheres or the vermis (Pomeroy et al., 2002; Schüller et al., 2008). This subgroup has the second-highest prevalence (25%) in patients and approximately 15-20% of SHH MB cases are metastatic with a local recurrence (Kuzan-Fischer et al., 2018; Luzzi et al., 2020). The potential for metastatic tumours to develop, as well as their association with TP53 mutations (13%), assign SHH MB to a "standard risk" category; 5-year survival rates are approximately 70% (Luzzi et al., 2020; Ramaswamy et al., 2016). More than half of the recorded cases occur in both infants and adults, with only about 14% of in children, so a bimodal age distrubtion scatters occurrence bewtween <5 and >16 years old (Kool et al., 2012; Luzzi et al., 2020). The paticular driver mutations that define the presence of an SHH MB tumour, all strongly correlated to the maintenance and regulation of the SHH pathway, are: TERT (83%), PTCH1 (45%), TP53 (13%), SUFU (10%), SMO (9%), MYNC (8%), and GLI2 (5%). Other prognostic factors for SHH MB are large cell anaplasia (LCA) and a loss of 9q (at the PTCH1 locus) (Kool et al., 2012). LCA SHH MB is mostly observed in children (22%) and infant (17%) cases; its presence predicts poor outcomes for these patients (Kool et al., 2012). Another histological diagnositic factor for SHH MB is the presence of desmoplastic tumours (16%), which is induced by the loss of function mtuation on Ptch1, correlated with positive survival outcomes (Kool et al., 2012). All adult SHH MB tumours to date have fallen into this histopathology category. All in all, the accumualted mutations,

potential for metastasis, histophatology and crhomosomal aberration make SHH the only MB subgroup with four independent diagnostic factors (Kool et al., 2012).

2. Cerebellum Development & SHH Pathway

2.1 Embryonic Cerebellar Development

During early embryonic development, the area where the cerebellum will generate, the anlage, is located in the segmental phase of the hindbrain (Butts, Green, & Wingate, 2014). A system of coordinated neurogenic patterning and cell movements aid in producing the cerebellar cortex and nuclei throughout embryogenesis. The signal for cerebellum development to begin is the establishment of the mid / hindbrain boundary at the neural plate; the isthmic organizer (IsO), a transient embryonic signaling center, secretes molecules along the anterior-posterior axis of the expanding neural tube to segment the necessary area for the cerebellum anlage (Harada, Sato, & Nakamura, 2016). In mice, this occurs during embryonic day 8.5 (e8.5) (Manto & Huisman, 2018). The roof of the hindbrain then establishes a dorsal-ventral signaling center at e10.5 within the anterior of the hindbrain (Butts et al., 2014; Manto & Huisman, 2018).

During e10.5 in mice, the dorsomedial ventricular zone (DZ) is established within the fourth ventricle of the embryo (Roussel & Hatten, 2011; Sudarov et al., 2011). This region will eventually give rise to all the necessary GABAergic neurons for cerebellum maturation. The cell types produced in this layer in are, in the following order of temporal generation, GABAergic cerebellar nuclei neurons, Purkinje cells, and PAX2-expressing cerebellar inhibitory interneuron progenitors (PIPs) (which later differentiate into the interneurons of the cerebellar cortex) (Manto & Huisman, 2018). Purkinje cells generated from the ventricular zone are also defined by the expression of Oligodendrocyte-specific bHLH

transcription factor (Olig2) (Manto & Huisman, 2018). With the help of a diverse pool of cerebellar interneurons, Purkinje cells carry the important responsibility of attenuating the output of cerebellar granule neurons (Manto & Huisman, 2018; Roussel & Hatten, 2011). Bergmann glia, an essential cell for the migration of cGNPs during cerebellum development, are generated from the radial glia that line the ventricular zone at e13.5 in (Sudarov & Joyner, 2007). Once Bergmann glia are present in the ventricular zone, they form a scaffold for the Purkinje cells to migrate toward the Purkinje Cell plate (Manto & Huisman, 2018). Between E11 and E14, the postmitotic precursors for the Purkinje neurons migrate away from the VZ to assemble at the core of the anlagen and form their own cell layer (Morales & Hatten, 2006). Bergmann glia have also demonstrated as having an active role in the direct the migration of molecular layer interneurons as well as cerebellum granule cell migration (Manto & Huisman, 2018). In rodents, the number of Bergmann glial fibers increases significantly during the first two postnatal weeks in mice (particularly due to the peak proliferation and migration of cGNPs) (Manto & Huisman, 2018). Like PAX2, Ptf1a expression is also necessary for the generation of GABAergic derivatives via the ventricular zone (Yamada et al., 2014). The interactions between PTF1A and ATOH1 maintain the interfaces of the ventricular zone and rhombic lip separate throughout embryogenesis and post-natal development (Yamada et al., 2014). Many of the necessary gene expressions for ventricular zone output, however, remain to be defined (Manto & Huisman, 2018).

Foundations for the rhombic lip, the second of the cerebellum germinal zones, is subsequently formed between the cerebella ventricular zone and the dorsal roof plate (Manto & Huisman, 2018). Glutamatergic neurons migrate along the top of the anlage and form the EGL by e11.5 (Manto & Huisman, 2018). This area will eventually produce 3 major glutamatergic neuronal subtypes that are derived in overlapping waves of neurogenesis

during postnatal expansion. At e12.5, cerebellar nuclei projection neurons migrate posteriorly from the rhombic lip (V. Y. Wang, Rose, & Zoghbi, 2005). By e13.5, the rhombic lip gives rise to unipolar bush cells (UBCs) that settle into the white matter of the IGL (Englund et al., 2006). The roof plate also expresses BMP signaling that induces the rhombic lip to express atonal homologue 1 (Atoh1); eventually cells expressing Atoh1 / Math1 emerge along the anterior aspect of this germinal zone (Chizhikov et al., 2010). The Atoh1 homologue is expressed in all of the rhombic cell derivates and is currently the only gene known to be necessary for the generation of its cell types (Manto & Huisman, 2018). Temporal expression of different proteins within the rhombic lip contribute to the cell-specific morphogenesis and migratory pathways as cells exit the germinal space towards their differentiated cell fate (Englund et al., 2006). One such temporally expressed protein is PAX6 which is present in all rhombic lip cell derivatives and regulates cGNP pre- and post-mitotic migration (Swanson & Goldowitz, 2011; Yeung, Ha, Swanson, & Goldowitz, 2016). An additional protein found in all rhombic lip cell lineages is ATOH1. However, there is no current knowledge that it helps to regulate rhombic lip cell lineage identity as previous experiments have determined that cell fate identify is designated to cGNPs before ATOH1 is expressed (Manto & Huisman, 2018). As the proliferating pools of progenitors continues to expand, the cells begin to migrate beyond the rhombic lip to spread across the surface of the cerebellar anlagen where they form the external granule layer (EGL) due to the presence of SDF1a activating their CXCR4 receptor (Haldipur et al., 2017; Roussel & Hatten, 2011). At E15.5, the cGNPs become post-mitotic cGNPs migrate radially across the surface of the anlagen then shift to migrating inwards towards the area ventral to the PCL to form the internal granule layer (IGL) (Roussel & Hatten, 2011). The IGL is an important location for adult cerebellum differentiation as it will hold the most abundant neuron of the brain: cerebellar granule cells.

Out of all the neurons that humans will produce, cerebellar granule neurons comprise 40% of the entire neuronal population (Roussel & Hatten, 2011). Despite the human cerebellum occupying 10% of all the allotted cerebral volume, it contains the vast majority of all the neurons associated with the CNS (Azevedo et al., 2009). To accommodate the dramatic expansion in the limited space of the posterior fossa, the anterior / posterior axis increases its folia by a multiple of 17.6 between e17.5 and P14 (Manto & Huisman, 2018). This is the favourable location for cerebral folding, which is a highly conserved feature in all mammals, as it provides space for the anterior / posterior outward-oriented cell division driven within the EGL.

2.2 Sonic Hedgehog Signaling

The Sonic hedgehog pathway is known for its key role in organogenesis, homeostasis, and regeneration during early developmental stages in mammals (Carballo, Honorato, & de Lopes, 2018). To carry out this role, Shh promotes nervous system cell type specification and provides the instructions for neural progenitor cell patterning into six different cell types (such as interneuron progenitors and motor neurons) via a Shh gradient (Carballo et al., 2018). When the SHH pathway becomes thrown into disarray tumorigenesis occurs and such is the case with medulloblastoma. In order to understand the key role this pathway presents for SHH MB genesis, its activity throughout normal cerebellum development must be understood. Current literature includes three classifications of HH homologous pathways in mammals: Desert (DHH), Indian (IHH), and Sonic (SHH). The most well studied in humans, in relation to disease, and especially MB, is SHH. During embryogenesis, the SHH pathway plays an important role in determining cell fate, the extent of proliferation for cells in the brain and spinal cord, limb and internal organ patterning, height of the organism, and stem cell maintenance (Carballo et al., 2018). When Shh is involved in cell fate it does so in a

concentration dependent manner; duration of cell exposure to Shh plays a key role (Ahn & Joyner, 2005).

MB Tumours secret Shh ligands in a paracrine manner that is either ligand dependent or receptor induced (Ahn & Joyner, 2005; Carballo et al., 2018). When Shh, a glycoprotein, is not present, Ptch1 12-transmembrane protein binds to Smo and inhibits the downstream cascade that would activate the SHH pathway. The beginning of the Shh signalling cascade occurs when extracellular Shh is present and binds to the Ptch1 receptor on the cell's surface (Fig. 2) (Carballo et al., 2018). Following this binding, Ptch1 becomes internalised into the cell and Smoothened Protein (Smo), a G protein coupled receptor, can no longer be inhibited by Ptch1 (Carballo et al., 2018). Smo then accumulates and stabilises at the primary cilium (PC) of the cell and proceeds to regulate Gli zinc-finger transcription factors processing and activation in the PC (Ahn & Joyner, 2005; Carballo et al., 2018). Once the Shh pathway is activated, within the target cell Gli transcription factors are translocated to the nucleus in order to activate Shh associated target genes (Carballo et al., 2018). The genes in question include Ptch1 (which activates a negative feedback loop for the Shh pathway) and Gli1 (a positive feedback loop) (Carballo et al., 2018). These SHH regulatory processes are subdivided between three Gli transcription factors (1, 2, and 3); each one regulating a separate portion of the SHH pathway (Carballo et al., 2018). Gli 1 acts as a full transcription activator for Shh associated genes (Manto & Huisman, 2018). When Gli1 is acetylated at Lysine 518, it leads to transcriptional deactivation of the Shh pathway. Both Gli2 and Gli3 have two different forms, activated or repressed, which are determined by post-transcriptional and post-translational processes (Carballo et al., 2018). Shh promotes proliferation of cGNPs in the ventral spinal cord during early development by inhibiting Gli3 (Manto & Huisman, 2018). The SHH mitogen then uses either Gli^{A} to activate, or Gli^{R} to repress, its pathway in

order to control cellular expression of distinct homeodomain proteins throughout different progenitor cell populations (Ahn & Joyner, 2005).

In response to Shh binding to Ptch1, Gli2 adjusts into its transcriptionally activated form (Gli2A) (Manto & Huisman, 2018). Gli2A begins to accumulate in the PC and is carefully regulated through the acetylation on Lysine 757 (Carballo et al., 2018). Gli3, on the other hand, is generally used as a transcriptional repressor (Gli3R) for the activated Shh pathway (Manto & Huisman, 2018). When Shh is not present at the cell's surface it is converted to its activated form (Gli3A), and Smo is freely expressed through ubiquitination (Manto & Huisman, 2018). The Gli transcription factors are also regulated in turn by the Suppressor of Fused (SUFU) protein whose job it is to negatively regulate the SHH pathway (Manto & Huisman, 2018). When Shh is not present and Ptch1 blocks Smo activation, SUFU binds to the Gli transcription factors and inhibits their translocation to the nucleus (Carballo et al., 2018). Gli is then converted to a C-terminal repressor (Gli-R) and suppresses the translation of Shh target genes. The truncated Gli form is then partially degraded by CK1 and PKA phosphorylation (Carballo et al., 2018; Iacovelli et al., 2006).

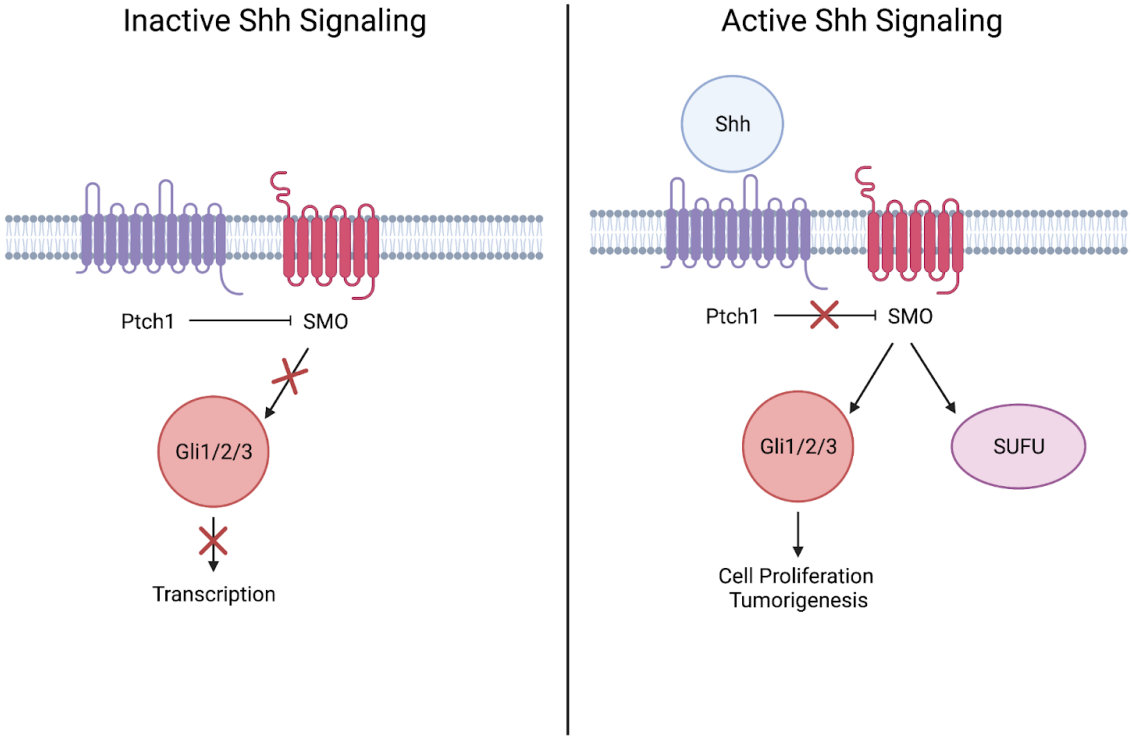

Fig. 2 | Model of the Shh pathway When Shh is not present and Ptch1 blocks Smoothened Protein (Smo), activation, a G protein coupled receptor, SUFU binds to the Gli transcription factors and inhibits their translocation to the nucleus. The beginning of the Shh signalling cascade occurs when extracellular Shh is present and binds to the Ptch1 receptor on the cell's surface. Following this binding, Smo, is no longer inhibited by Ptch1. Smo then accumulates and stabilises at the primary cilium (PC) of the cell and proceeds to regulate Gli zinc-finger transcription factors processing. The target cell Gli transcription factors are then translocated to the nucleus in order to activate Shh associated target genes. Created with BioRender.

2.3 Postnatal Cerebellum Neuronal Generation

Once the embryonic cell layers of the cerebellum are established and the mouse is born, a series of crucial postnatal processes must occur to ensure proper neurogenesis and development of the cerebellum. During the post-natal stages, the cerebellum is defined by three cell layers established throughout embryogenesis: the EGL, the Purkinje cell layer, and the IGL. Specific cell types were prenatally allocated along the dorsal ventral axis and cell

type allocation extends into mammalian postnatal life (P21 for mice and up to 2 years postnatal in humans) (Butts et al., 2014). Other factors in the extracellular matrix of the EGL regulate proliferation, such as the expression of F3/contactin which suppresses Shh-dependent proliferation (Butts et al., 2014). Premature misexpression of F3 / contactin in the postnatal cerebellum may lead to attenuating granule cell progenitor proliferation (Butts et al., 2014). This phenomenon highlights how the EGL, outside of Shh stimulation, plays an important role in cGNP expression and cerebellum development.

In early post-natal stages (P0-P14 in mice), Shh signaling is a primary driver of the dramatic expansion of the cGNP precursor pool (Manto & Huisman, 2018). Other proliferative mitogens that are indicated in the EGL's post-natal expansion are Wnt5a, insulin-like growth factor (IGF1), and NOTCH2 (Manto & Huisman, 2018). Furthermore, the EGL itself is subdivided into the outer (ext-EGL) and inner regions (int-EGL); the former containing a proliferative of cGNP populations while the latter is composed of postmitotic on the verge of migration (Butts et al., 2014). As the Shh pathway becomes highly expressed in embryonic tissue of the developing cerebellum, transit amplification of cGNPs in the ext-EGL is encouraged. From P2 – P4, the mouse cerebellum experiences an intense promotion of cGNP proliferation in the EGL due to the diffusion of the Shh mitogen from the PCL (Roussel & Hatten, 2011). The cGNPs that populate the ext-EGL reach peak proliferation in mice at P7; the EGL is at its thickest and millions of cGNPs can be harvest from one mouse alone (Manto & Huisman, 2018; Roussel & Hatten, 2011). Cells in this state also express the basic helix-loop-helix (bHLH) transcription factor Atoh1 / Math1 that is required for transient proliferation and suppression of differentiation (Flora, Klisch, Schuster, & Zoghbi, 2009; Klisch et al., 2011). This proliferation stage of neural development requires extreme care and regulation as, in mammals, the cerebellum contains over half of the mature neurons in the

adult brain that are generated via this pathway (Butts et al., 2014). By the end of the 2nd postnatal week in mice, and at 30-40 postnatal weeks in humans, the cGNPs begin to exit the cell cycle and migrate into the int-EGL (Manto & Huisman, 2018). Using the Bergmann glia fibers extending from the IGL, the postmitotic cGNPs extend their parallel fibers and begin to migrate tangentially (Roussel & Hatten, 2011; Volpe, 2009). As cGNPs exit the cell cycle, they upregulate $P27^{Kip1}$, a tumour suppressor cyclin dependent kinase inhibitory protein (Ayrault, Zindy, Rehg, Sherr, & Roussel, 2009; Helms, Abney, Ben-Arie, Zoghbi, & Johnson, 2000). After P7 in mice, and 10 weeks in postnatal humans, the cGNPs in the int-EGL shift to itinerate radially towards the IGL within the cerebellum parenchyma (Holgado et al., 2017; Manto & Huisman, 2018). Meanwhile, cGNPs that remain in the outer-EGL, furthest from the Shh gradient, continue to expand over (Butts et al., 2014; Fujita, 1967; Kool et al., 2012; Lewis, Gritli-Linde, Smeyne, Kottmann, & McMahon, 2004).

The Shh mitogen uses multiple mechanisms at its disposal in order to control cGNP proliferation. One such method is through the modulation of cell cycle regulators cycle D1 (Ccdnd1) and Ccnd2 (Kenney & Rowitch, 2000). Early post-natal cGNPs express Ccnd1 and Ccnd2 while a pool of progenitors are generated during peak cGNP neurogenesis (such as P7 in mice) and Ccnd2 (Roussel & Hatten, 2011). Ccnd1 activation is quite necessary for the required cGNP needed for cerebellar development as mice that lack *Ccnd1* experienced slower cGNP proliferation and cerebellar development (Pogoriler, Millen, Utset, & Du, 2006). Mice lacking both Ccnd1 and Ptch1 also exhibited reduced incidences of medulloblastoma suggesting that the control of Ccnd1 expression may be a method of suppressing Shh medulloblastoma formation (Pogoriler et al., 2006). Shh also activates, and regulates, the proto-oncogene MycN (Kenney, Cole, & Rowitch, 2003). When overexpressed, MycN promotes the upregulation of Ccnd1 mRNA (Kenney et al., 2003). Notch2, a transmembrane protein aids in determining cell fate decisions during development, by

stimulating cGNP proliferation and inhibiting granule neuron differentiation (Solecki, Liu, Tomoda, Fang, & Hatten, 2001). Upon cGNPs exposure to Notch2, or any activated form of the receptor, the cells experience a 3-5x increase in proliferation as well as an overexpression of the HES1 transcription factor (also induced along the Shh pathway) (Solecki et al., 2001). Once the post-mitotic progenitors have reached the IGL, they become differentiated neurons and form synapses (Butts et al., 2014; Fujita, 1967; Kool et al., 2012; Lewis et al., 2004). The factors governing how long progenitors navigate this environment and terminate transient proliferation is not clearly defined yet equally important for understanding CNS development and disease.

As an imbalance of cGNP proliferation, or differentiation, can cause hypoplasia or tumour formation, proper check stations must be in place to ensure only the adequate number of granule cells are generated and differentiated to ensure proper cerebellum morphogenesis (Manto & Huisman, 2018). The EGL is also physically limited in its capacity to contain neural progenitors and the total number of cGNPs necessary for hindbrain development cannot all proliferate, migrate, and differentiate in one fell swoop (Butts et al., 2014). The cellular capacity of the EGL is reached at 34 days in postnatal humans yet it will continue to host proliferating cGNPs for the next 2 years (Butts et al., 2014; Rahimi-Balaei, Bergen, Kong, & Marzban, 2018). Antagonists of Shh-mediate cGNP proliferation act as negative regulators for the progenitors' expansion in the cerebellum. The pathways that help to negatively regulate Shh-stimulated proliferation are BMP4, WNT3, and Anaphase-promoting complex / cyclosome (APC / CCDH1) ubiquitin ligase (Manto & Huisman, 2018). These antagonists include bFGF as well as BMP2 and BMP4, the latter two being expressed solely in post-mitotic, differentiating cGNPs in the int-EGL (Fogarty et al., 2007; H. Zhao, Ayrault, Zindy, Kim, & Roussel, 2008). Both BMP2 and BMP4 act to inhibit Shh-induced

proliferation via a Smad signaling pathway (H. Zhao et al., 2008). More precisely, Bmp4 antagonises Shh signaling and induces cGNP differentiation via the rapid posttranscriptional turnover of the Atoh1 / Math1 gene (Ayrault et al., 2010). By the end of the first postnatal year in humans, and P21 in mice, the EGL dissipates, the cGNPs begin to experience a dramatic decreased response towards the Shh mitogen (despite there being no change in the Shh gradient produced by the PCL), and the IGL continues to increase in size as cerebellar circuitry matures (Ahn & Joyner, 2005; Volpe, 2009).

Although many additional pathways have been implicated in the multiple tangential and radial phases of the granule cell migration, the mechanisms that mediate the decision of individual granule cells to switch to their mode of migration, exit the cell cycle, and become unresponsive to Shh are poorly understood. One proposed model to explain this phenomenon is that diminishing Gli activity is a contributing factor as its rate of disappearance is inversely proportional to the initial concentration of the Shh mitogen (Ahn & Joyner, 2005). Epigenetic modifications of Gli genes, which act as downstream Shh effectors, have also been shown to exhibit negative regulation on cGNP proliferation (Zanin, Abercrombie, & Friedman, 2016). Deacetylation of the regions surrounding Gli1 and Gli2 transcription factors has been demonstrated to maintain the cGNPs postmitotic state (Canettieri et al., 2010). However, more work must be conducted to hone the specific causes of this important stage in neural development.

2.5 Cell Specification and Patterning in the Cerebellum

Once proliferation and the migration towards differentiation has been completed in the following stages of neural development are necessary breadth of cellular diversity required for cerebellar functioning. This temporally, and spatially, refined process is what provides

mammals with functional neural circuitry. As the cerebellum is the primary center for motor coordination, the organisation of its cytoarchitecture is incredibly important for survival. From superficial to deep, the highly conserved cytoarchitectural features of the mammalian cerebellum are the molecular layer, the Purkinje cell layer, and the granule layer (Manto & Huisman, 2018). In the adult cerebellum, areas of white matter contain three pairs of cerebellar nuclei made up of glutamatergic projection neurons and GABA-expressing interneurons (Sudarov et al., 2011). The IGL is composed of glutamatergic granule cells as well as a variety of scattered interneurons while the adjacent PCL holds the cell bodies of GABAergic Purkinje cells and Bergmann glia (Sudarov et al., 2011). Once the EGL disappears, the fully developed outer layer of the cerebellum contains three types of interneurons (candelabrum, basket, and stellate) as well as Purkinje cell dendrites and glutamatergic cell axons (Sudarov et al., 2011). In the ventricular zone of the cerebellum, Ptf1a expression leads to the generation of excitatory GABAergic interneurons (Hoshino et al., 2005).

As for inhibitory glutamatergic cells, they are derived from Atoh1 expressing cells located between the ventricular zone and the roof plate (Rose, Ahmad, Thaller, & Zoghbi, 2009). Unlike cGNPs, these cells exit the rhombic lip as postmitotic newly differentiated neurons. The first few glutamatergic cells express LHX9+ and are destined to form the lateral nucleus projecting information to the midbrain and thalamus (Green & Wingate, 2014). The cells that are produced express TBR1+ and form the medial cell group sending their axons towards the hindbrain (Green & Wingate, 2014). Previous work has also revealed the importance of Atoh1 and Ptf1a expression for cerebellum neural differentiation as a genetic deletion of either gene leads to increased mixing of cell lineages during postnatal mouse development (Millen, Steshina, Iskusnykh, & Chizhikov, 2014).

Purkinje cells, as previously indicated, are GABAergic neurons and therefore transmit inhibitory signals (Manto & Huisman, 2018). They are solely in charge of receiving the outflow of information from the cortex which they then transmit to cerebellar nuclei as an inhibition projection (Manto & Huisman, 2018). The fan-like dendritic trees that extend from Purkinje cells spread dorsally towards the cerebellum's most superficial layer, the molecular layer (Manto & Huisman, 2018). In this region, Purkinje cell extensions receive two types of input: direct and indirect (the latter being the most numerous source of input in the cerebellum) (Manto & Huisman, 2018). These cells will also form synaptic junctions with granule cells within the molecular and granule layers of the cerebellum (Manto & Huisman, 2018). Throughout the first postnatal week in mice, the inhibitory interneurons within the white matter of the cerebellum remain proliferative (Leto, Carletti, Williams, Magrassi, & Rossi, 2006). Eventually, environmental cues will arrest mitotic activity and the interneurons will differentiate (Manto & Huisman, 2018). Mature inhibitory interneuron progenitors use a novel pathway to reach their mature, interneuron phenotype compared to other cerebellum progenitors; within the white matter their acquire their fully developed form postmitotically rather than through active cell division (Leto et al., 2006). The characteristics associated with these GABAergic interneurons (stellate, basket, and Golgi cells) are inhibitory transmissions (like the Purkinje cells) and the use GABA as their primary NT. The one exception is that Golgi interneurons use both glycine and GABA as their NT (Manto & Huisman, 2018).

The excitatory neurons within the cerebellum, granule cells use glutamate for neurotransmission (Manto & Huisman, 2018). Granule cells are also the most numerous cell population in the mammalian CNS; the adult human brain will contain approximately 10^{10} – 10^{11} post-development (Manto & Huisman, 2018). The unmyelinated granule cell axons project into the molecular layer of the cerebellum where they form parallel fibers and en

passant synapses within dendritic trees extending from the Purkinje cell layer (Manto & Huisman, 2018).

2.6 SHH Mitogen and Medulloblastoma

The timing of cGNP migration outside of the EGL is heavily regulated and genes that modify this phenomenon have a potential importance in medulloblastoma tumorigenesis. Mice with loss of function mutations on CXR4 experience a lack of dramatic cellular expansion in the cerebellum which is necessary for development as well as premature migration of cGNPs from the EGL (Carballo et al., 2018). Mutations in Purkinje cells can also lead to cerebellar patterning defects. For example, BDNF is an important protein released by the Purkinje cells which promotes the migration and differentiation of cGNPs from the EGL (Borghesani et al., 2002). However, when mice are generated with mutations on BDNF impairing protein function, the rodents experience severe defects in cerebellar patterning (Borghesani et al., 2002). As previously stated, Purkinje cells also secrete the Shh mitogen within the developing cerebellum and the constitutive activation of Shh signaling via mutations within these cells will not soley induce MB tumorigenesis; secondary tumour suppressors, such as TP53, must be deactivated as well (Carballo et al., 2018). However, other downstream mutations along the canonical and noncanonical Shh pathway such as those on Ptch1 (the transmembrane protein receptor for Shh) and SUFU (a negative regulator of Shh signaling) are capable of exclusively promoting a tumorigenic environment in the cerebellum (Carballo et al., 2018). Using in vivo models, Carballo et al. even demonstrated a strong correlation between Ptch1, Gli1, and Gli2 mRNA expression that coincided with canonical Shh pathway activation and tumorigenesis (Carballo et al., 2018). The activating mutations for Gli1 and Gli2 promoted a fluctuation of their active forms (Gli^A) and, combined with the suppression of the Ptch1 transmembrane protein, lead to the over-proliferation of cGNPs in the EGL (characteristic of Shh MB) (Carballo et al., 2018). Despite this, not all Gli^A dysfunction is

essential for Shh-dependent cell proliferation pathways. Studies conducted within the past decade have also revealed Shh's important role as a promoter for tumour microenvironment formation in MB (as well as basal cell carcinoma) (Cohen Jr, 2003).

As previously mentioned, mutations along p53 have been correlated to the generation of SHH MB tumours. The role of p53 is commonly known as a tumour suppressing protein that surveys genetic instability in mitotic cells. When properly implemented, p53 will induce cell cycle arrest, senescence, and apoptosis in order to discard potentially oncogenic mutations in proliferating cells. Due to its role as a guardian against protooncogenes, p53 mutations are oftentimes observed in human cancers. Its role in the developing cerebellum, however, is not widely understood. Current literature states that p53 acts as a negative regulator of Gli proteins so it can downregulate Shh induced proliferation during development (Barthelery & Manfredi, 2016). Conversely, Shh signaling from the Purkinje cells inhibits p53 activity through the activation of negative p53 regulator Mdm2 (an E3 ubiquitin ligase) (Barthelery & Manfredi, 2016). Mdm2 regulates p53 via proteasomal degradation (Liu et al., 2009). This E3 ligase can also receive aid from its counterpart, Mdm4, as a transcriptional repressor for p53 (Barthelery & Manfredi, 2016). In SHH MB, the modification to the regulatory relationship between p53, Mdm2 and Mdm4 has been implicated in tumorigenesis. An *in vivo* experiment conducted by Barthelery et al. they added both Mdm2 and Mdm4 to mouse embryos and, upon observing pre- and post-natal stages of development, found that their mice experienced a significantly reduced cGNP differentiation and overall development of the cerebellum (Barthelery & Manfredi, 2016). Likewise, when mice were genetically modified for a homozygous loss of function mutation on Mdm2 and Mdm4, the mouse embryos could not live past e4.5 (Parant et al., 2001). Even heterozygous mouse mutants experience decreased cerebellar foliation (Barthelery & Manfredi, 2016). The only method to recover the mouse

models, for both cases, was to add an additional homozygous or heterozygous p53 mutation, respectfully (Barthelery & Manfredi, 2016).

2.7 Effects of Glutamate on Medulloblastoma

In the case of SHH MB, mutations that lead to the overactivation of Smo stimulate uncontrolled cell proliferation, i.e., tumorigenesis, during cerebellum development in mammals. Previous work by Iacovelli et al. demonstrated that upon the addition of Smo inhibitor to cGNPs with Smo activating mutations, cell proliferation was inhibited and high rates of apoptosis in SHH MB cells were observed (Iacovelli et al., 2006). Furthermore, subsequent in vivo experiments linked the effects of Smo inhibitors to a glutamate receptor, mGlu4 (Iacovelli et al., 2006). This evidence identified the potential of G-protein coupled receptors as a novel target to curb burgeoning numbers of SHH MB cells in patients. More importantly, mGlu4 receptors are also expressed by proliferative cGNPs which, as was previously stated, are the cells of origin for SHH MB (Canudas et al., 2004). In these cerebellar progenitors, mGlu4 inhibits the release of glutamate (an excitatory NT), in parallel with fiber-Purkinje cell synapses in the molecular layer of the cerebellum to support neuronal survival. Previous *in vitro* experiments where mGlu4 was activated in SHH MB cell lines demonstrated an inhibition of the PI-3-K pathway and a reduction in proliferation (Iacovelli et al., 2006). In contrast, when the PI-3-K pathway is activated via glutamate, cell survival and proliferation is promoted (Canudas et al., 2004). Since over proliferation is a tumourigenic event in SHH MB, the use of mGlu4 to inhibit such processes could lead to interesting areas of treatment for MB patients. Glutamatergic inhibition of the PI-3-K pathway occurs in the extracellular environment and when stimulated *in vitro*, encourages differentiation of SHH MB samples (Pazzaglia et al., 2006). This experiment expanded upon prior implications that the mutations affecting the regulation of the PI-3-K pathway act as a

pillar for MB tumor formation (Pazzaglia et al., 2006). Additional experiments injecting Ptch$^{-/+}$ mice with PHCC (a PI-3-K inhibitor), an mGluR4 receptor agonist, dramatically decreased MB tumour growth curves as well as a decline in the over proliferation of cGNPs (Pazzaglia et al., 2006). An important note to mention is that despite mGlu4's ties to the Shh pathway and glutamate's negative influence on the PI-3-K pathway, activation of the mGlu4 receptor does not directly interfere with either the SHH or WNT pathways (Canudas et al., 2004). This phenomena proposes a model wherein the antiproliferative actions of mGlu4 activation on SHH MB tumour cells is an upstream obstruction to the PI-3-K pathway (Canudas et al., 2004). Using Ptch$^{-/+}$ mice, Canudas et al. were able to link high cerebellar activation of the PI-3-K pathway and support the survival of cGNPs carrying DNA damage due to irradiation treatments during early brain development (Canudas et al., 2004). Therefore, the connection of this data to current literature that suggests glutamate, and its subsequently activated pathways, acts as a novel avenue of therapy that could eliminate SHH MB mutated cells and limit early tumorigenesis via inhibition of the PI-3-K pathway.

3. Neural Activity in Medulloblastoma and the Central Nervous System

3.1 How Membrane Potential Is Used to Develop the CNS

Throughout the course of cerebellum development, as well as the day-to-day processes of the adult brain, the regulation of membrane potential is quite important. Whether the cell is in an excitable or non-excitable state can instigate cell cycle initiation during early mammalian development of the CNS. NT, such as GABA and Glutamate, depolarise cells in the ventricular zone of the brain all through the early stages of neurogenesis and cause the cell to become excitable (LoTurco, Owens, Heath, Davis, & Kriegstein, 1995). Glutamate acts upon AMPA receptors; ionotropic receptors which are heterotetrametric complexes located in all regions of the mammalian brain (Y. Zhao, Chen, Swensen, Qian, & Gouaux, 2019). When

the receptor is activated by glutamate, its Glu 1-4 subunits carry out their designated roles to induce cell excitability (Hollmann & Heinemann, 1994). This activation allows for Na^+ and K^+ ions to pass through the cell membrane due to their ability to quickly open and close as AMPA receptors are also responsible for some of the fastest synaptic transmissions in the nervous system (Platt, 2007). The presence of glutamate also alters the cell membrane so it can no longer be permeable to $Ca2^+$, differentiating in function from N-methyl-D-aspartate (NMDA) (another ionotropic glutamate receptor in the CNS). NMDA receptors are located on neurons of the CNS, specifically in the dendritic spines. In order to become activated, NMDA requires multiple conditions to be met simultaneously, such as the removal of Mg2+ and Zn 2+ once the neuron is depolarised, to allow cations to pass through the cell membrane (Furukawa, Singh, Mancusso, & Gouaux, 2005). Nevertheless, once glutamate activates either AMPA or NMDA, the cell potential reaches 0 mV, becomes depolarized, and contributes to postsynaptic activation and synaptic plasticity (Platt, 2007).

GABA receptors are in every region of the brain. Their presence is important for neural development as GABA plays a key role during early embryogenesis; in the mammalian CNS, GABA acts as the primary inhibitory NT and works in tandem with glutamate to regulate neural processes. GABA receptors are divided into two classes, $GABA_A$ (ionotropic) and $GABA_B$ (metabotropic) (C. Wu & Sun, 2015). The former subclass act to quickly hyperpolarise the cell via the opening of ion channels that allow Cl^- entry into the cytoplasm. The localisation of mature $GABA_A$ receptors also depend on their subtype classification (α, β, γ) (C. Wu & Sun, 2015). α1and α2 subunits are found in the synaptic clef whereas α4, 5, 6, and γ are only localised to the presynaptic region of the neuron. $GABA_B$ receptors, on the other hand, enact much slower transmissions; they are responsible for a slower inhibitory message using secondary messengers (C. Wu & Sun, 2015). Once activated, $GABA_B$

receptors release G protein subunits causing a signalling cascade of K^+ channel activation or Ca2+ channel inhibition (C. Wu & Sun, 2015). Whichever way, GABA receptors are responsible for cell depolarisation events and inhibitory signal propagation.

In tandem, both GABA and Glutamate NT can produce an increase of intracellular $Ca2^+$ in neural cells. During embryonic development of the cerebellum, the GABAergic interneurons migrate into the cerebellar white matter where they receive environmental signals to help dictate cerebellar progenitor differentiation (Leto et al., 2009; C. Wu & Sun, 2015). Another study conducted by Dhar et al. demonstrated that immature granule cells of the cerebellum depend on GABAergic synapses for appropriate dendritic development (despite there being an equal number of glutamatergic synapses) (H. S. Venkatesh et al., 2015). This portion of dendritic development is important for the adult cerebellum as the extending dendrites are responsible for receiving both excitatory and inhibitory signals (H. S. Venkatesh et al., 2015). Within the cytoarchitecture of the developing cerebellum, the distribution of GABA and glutamate is also uneven; the IGL contains a higher concentration of glutamates whereas the EGL has a lower amount (Holgado et al., 2017). This is especially interesting as the IGL contains the differentiated cGNPs and the EGL is the location of cGNP proliferation demonstrating that these neurotransmitters might enact cell cycle events in a concentration dependent manner; an assumption compounded by previous experiments which demonstrate how the addition of either GABA or Glutamate *in vitro* lead to a decrease in DNA synthesis (i.e., an increase in cell cycle exit) (Holgado et al., 2017). These results furthered the idea that NT influences on neocortical progenitors in their proliferative state help regulate neocortical neurogenesis.

3.2 Cases of Neural Activity in Neuro-Oncology (CNS)

The potential role that neural activity might play in SHH MB tumorigenesis is not a novel idea, especially when it is compared to other cancers in the CNS. For example, elevated premotor cortical projection neuronal activity leads to an increase in glioma cell proliferation as well as an overall increase in *in vivo* tumour growth (H. S. Venkatesh et al., 2015). An additional study conducted on adult and paediatric high-grade gliomas (HGGs) by Venkatesh et al. demonstrated that post-optogenetic stimulation of the cortical tissue, 9/10 HGG patient samples experienced an increase in proliferation (H. S. Venkatesh et al., 2015). This phenomena was found to be specifically mediated by BDNF and neurogligin-3 (NLGN3) and, in other cases, BDNF has been known to promote oligodendrocyte precursor cell (OPC) proliferation and myelination (Wong, Xiao, Kemper, Kilpatrick, & Murray, 2013). OPCs are the most proliferative cell population in the adult brain and are postulated to be the cell of origin for many high-grade glioma tumour subtypes (H. Venkatesh & Monje, 2017). Glioblastoma cells are also associated with secreting a high volume of glutamate *in vitro* leading to their tumour, as well as the surrounding tissue, experiencing an increase in glutamate concentration; the tumours that secreted more glutamate experiencing a better growth advantage *in vivo* (Takano et al., 2001; Ye & Sontheimer, 1999). GABA is also present in glioblastomas yet experimental analysis of multiple patient-derived tumour cells found GABA to have both depolarizing or hyperpolarizing effects (Labrakakis, Patt, Hartmann, & Kettenmann, 1998). This phenomena appears to be dictated by intertumoral heterogeneity yet it remains poorly understood (Labrakakis et al., 1998). Another influential growth factor BDNF, has been found to produce an effect glioblastoma. Neuronal expression and secretion of BDNF influences diverse processes ranging from proliferation, cell survival, neural circuit development, and long term potentiation (Bartkowska, Paquin, Gauthier, Kaplan, & Miller, 2007; Hong, McCord, & Greenberg, 2008). In glioblastoma tumour cells,

BDNF mutations promote proliferation and survival of tumour cells through TrkB mediated signaling (Lawn et al., 2015). A correlation between BDNF over-activation and paediatric glioblastoma has also been strongly implicated as contributing to the over proliferative effects common in these tumour cells (H. S. Venkatesh et al., 2015; G. Wu et al., 2014).

3.3 Cases of Neural Activity in Oncology outside of the CNS

Neural activities proto-oncogenic effects are not only limited to MB or other cancers of the nervous systems, many of its mechanisms have also been linked with the development of non-nervous system organs (H. Venkatesh & Monje, 2017). As nervous system activity strongly modulates the function of stem and precursor cells as well as playing a multitude of roles in organ development, maintenance, plasticity, and regeneration in a diverse range of tissue; it is no surprise then that it has been postulated to have effects on tumorigenesis and cancer progression. In skin tissue, innervation occurs early in cutaneous morphogenesis and a paper published by Peterson et al. demonstrated that cutaneous nerves could be playing an important role in basal cell carcinoma (BCC) tumorigenesis (Peterson et al., 2015). The proliferation of follicular and touch stem cells of the epithelium, which are the cells of origin for BCC, is controlled via the Shh pathway. Ptch mutations in BCC lead to the continuous activation of the SHH pathway which, as it does in SHH MB, and the continuous innervation of Shh ligand-expressing sensory nerves in the epithelium drives BCC progression (Peterson et al., 2015). Specifically, Peterson et al discovered that the innervation of Gli1-expressing progenitors, a transcriptional regulator activated via the SHH pathway, was especially present in highly tumorigenic BCC cells (Peterson et al., 2015). Patients with Gorlin Syndrome (also known as Nevoid Basal Cell Carcinoma Syndrome) experience sustain germline mutations in Ptch1 in their epidermal tissue which predisposes them multiple cancers, including basal cell carcinoma (Pastorino et al., 2009). The innervation of sensory nerves within the epithelium

plays a key role in activating the SHH signalling for development whereas denervation attenuates over activation of the Shh pathway and tumorigenesis for BCC (Peterson et al., 2015).

Another example of proto-oncogenic effects of neural activity outside of the CNS can be found in bone tissue. Glutamate signaling plays an important role in osteoblast function and bone remodeling. Osteoblasts secrete glutamate in an autocrine / paracrine manner and when either AMPA or NMDA are coupled with the NT, this stimulates osteoblast maturation and bone formation (Hinoi, Fujimori, Takarada, Taniura, & Yoneda, 2002; Lin, Yang, Tang, Wu, & Fu, 2008). Stimulation of the NMDA receptor also induces c-fos expression, which is also used as a model for neural activity in the cerebellum later in this thesis, promoting osteoblast proliferation. This phenomenon has been linked to osteosarcoma initiation and could potential play a prominent role in bone cancer pathogenesis (H. Venkatesh & Monje, 2017). Osteosarcoma cells also contain multiple glutamate receptors (such as NDMA, NR1, NR2A, and NR2B and NR2D) but the metabotropic mGlur4 receptor was significantly present in both osteosarcoma (~20%) and benign giant cell tumours of bone tissue (40%); these findings strongly correlated to positive survival outcomes for osteosarcoma patients (Kalariti, Lembessis, & Koutsilieris, 2004; S. Wang et al., 2016). Muscle cells also heavily depend on electrical activity in everyday functioning; however, little is known about the role innervation plays in rhabdomyosarcomas. One paper by Chakroborty et al demonstrated that mice injected with sarcoma tumour cells into their thigh muscles, experienced stagnated tumour growth and progenitor cell mobilization following injections of dopamine (Chakroborty et al., 2008). Mice that were altered to not have dopamine receptors but were still injected with sarcoma tumour cells failed to produce any positive responses to the dopamine injections (Chakroborty et al., 2008). Prostate cancer cells also show an altered progression once

exposed to specific neurotransmitters. For example, cholinergic signalling through muscarinic receptors leads to cancer proliferation whereas adrenergic signalling promotes prostate tumour migration (Anderson, Hanlon, Patchefsky, Al-Saleem, & Hanks, 1998; Batsakis, 1985). When B2 and B3-adrenergic receptors were deleted from *in vivo* mouse models, poor prostate tumour engraftment and growth followed, however, the activation of cholinergic signalling via parasympathetic innervation promotes metastasis (Anderson et al., 1998; Batsakis, 1985). The mechanisms that mediate neuronal influences on cancer growth and progression are not fully understood, whether that be through nervous system tissue or not. Unveiling these contributions that neural activity might have on tumour progression might lead to novel therapeutic avenues.

3.4 Genetic & Epigenetic Events Converging on Neural Activity in Medulloblastoma

The process of directing pre- and postnatal neurogenesis induces the coordination of many biological pathways throughout development. SHH MB contains such errors in important developmental pathways leading to tumorigenesis. Many aspects of SHH MB tumorigenesis, such as the events behind sustained proliferation in the cerebellum, remain poorly understood. Unveiling the responsible mechanisms could lead to the discovery of novel therapeutic targets. Previous work in the Garzia lab has attempted to tackle this subject by analyzing the genetics of SHH MB tumour samples. The Garzia lab was able to derive a list of genes that had been mutated or silenced; by running an analysis of all the single nucleotide variants (SNVs) as well as a pathway analysis, the Garzia lab was able to sort for different themes amongst the mutated genes (Fig. 3A). The anticipated convergence on SHH pathway genes were present, however, an unexpected pattern was observed on mutations associated with electrical activity; genes linked to pre-synaptic membrane organisation and assembly were particularly present in the results (Fig. 3A). To probe this lead even further, the Garzia

lab wanted to test whether epigenetic modulators connected to neural activity development may play an important role in promoting SHH MB tumorigenesis. To conduct this screening, the Garzia lab ran a CpG methylation analysis on the promoters of all the genes in the patient samples and compared it with a list of hypermethylated promoters in other MB subgroups (Fig. 3B). Using this method, they could exclude overlapping patterns between the 4 MB subgroups and isolate which ones were novel interactions in SHH MB. This methylation profile corroborated the SNV screening; promoter hypermethylation and silencing in SHH MB tumours was occurring on genes negatively regulating potassium channel activity and membrane potential. From these results, the Garzia lab hypothesized that the regulation of neural activity was a central event exclusive to SHH MB tumorigenesis and that lack of ability to respond to neurotransmitter induced depolarization was predisposing cerebellum progenitors to malignant transformation. To demonstrate whether electrical activity and membrane depolarization influence medulloblastoma tumor cells, our lab developed an optogenetically modified mouse model of medulloblastoma. The model expresses the fast-gated blue-light controlled protein hChR2 under the control of an EGL specific promoter (Math1 promoter). These mice were crossed with ptc-/+ mice to generate tumor prone mice that would express hChR2 in the tumor cells. Repeated photostimulation in vitro and ex vivo (cells and organotypic slices) results in decrease of tumorigenesis. This suggests that membrane depolarisation is a form of non-genetic tumour suppressor mechanisms in medulloblastoma.

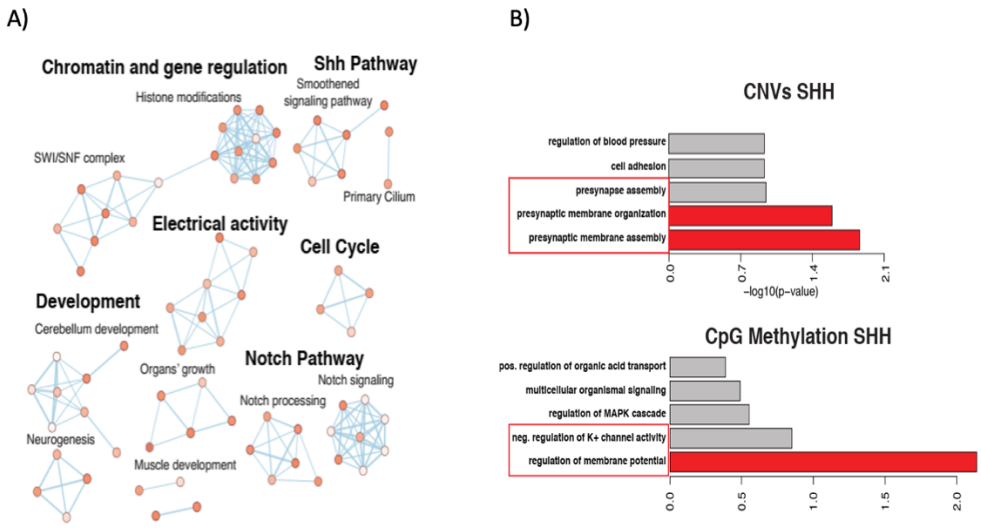

Fig. 3 | Genetic and Epigenetic Convergence of Neural Activity in Shh Tumours (A) Cytoscape enrichment map of a pathway enrichment analysis of recurrent somatic genetic events (SNVs and INDELs) in Shh medulloblastomas. (B) Significantly enriched pathways across single gene CNVs (top) and CpG hypermethylation loci in primary SHH medulloblastomas.

4. Rationale and Hypothesis

Given the above, I hypothesized that similarly to what happens in tumor cells, electrical activity mediated by neurotransmitters also affects the biology of Shh MB cells of origin, the cGNPS.

Chapter 2: Methods

1. Dissection of post-natal mouse cerebella

C57BL6 mice were euthanized on the postnatal day required for each experiment by decapitation under isoflurane anesthesia. Their brains were immediately removed and placed in Slicing Media (HBSS, 30mM D-glucose, 2.5 mM Hepes, 1mM CaCl2, 1mM MgSO4, 4mM NaHCO3) on ice. Cerebella were then isolated by inserting a pipette tip between the cerebellum and the colliculus and gently separating the two pieces. The brainstem was then similarly removed so only cerebellar tissue was used for the CGNP dissociation. Experiments were in accordance with policies of the Research Institute of the McGill University Health Center Animal Facility Guidelines and the Canadian Council on Animal Care.

2. Dissociation of cGNPs from dissected post-natal mouse cerebellum

cGNPs were dissociated from cerebella using the Papain Dissociation System (Worthington #LK003150). Steps 1 through 5 were followed as written in the Worthington protocol. Following these steps, 300µl of ovomucoid (from the Worthington kit) was added to the incubated dissociation tube. The tissue in the tube was then triturated with a pipette and the remaining undissociated tissue was allowed to settle to the bottom. The cloudy cell suspension was then collected in a clean 15ml Falcon tube. Trituration and collection were repeated until all the tissue was dissociated. The cell suspension was then poured through a 40µm sterile filter. The cell suspension was centrifuged at 200xg for 7 minutes to obtain a sample cell pellet which was stored at -20°C. The supernatant cell solution was used for cell culture experiments.

3. Treatment of 24-well TC plates for Cerebellar Culture Proliferation Experiments

A 24-well plate (Starstedt, Cat. No. 83.3922) was treated with Poly-D Lysine (Thermo Fischer Cat. No. A3890401) in order to encourage proper cell adhesion of cerebellar cultures. Each well was treated with 200 uL of 0.1mg/mL of Poly-D Lysine and incubated at room temperature for 1 hour. The Poly-D Lysine was then aspirated, and the wells were twice rinsed with 500 uL of ddH_2O. The plates were then left uncovered under the cell culture hood for approximately 1 hour prior to use.

4. Evaluation of P7 mouse cGNP proliferation in response to treatment with neurotransmitters

Cells were plated at $2x10^6$ cells /ml in Poly-D Lysine treated 24-well plates. Each well was supplemented with 1uM Sonic Hedgehog Signalling Agonist (SAG) , 1mM L-glutamate or 50uM GABA were added to their corresponding two technical replicates immediately after plating. In each experiment two wells per time point were treated with SAG alone as a positive control for proliferation. Every 24hrs, for 72 hours, cell counts were taken using a haematocytometer.

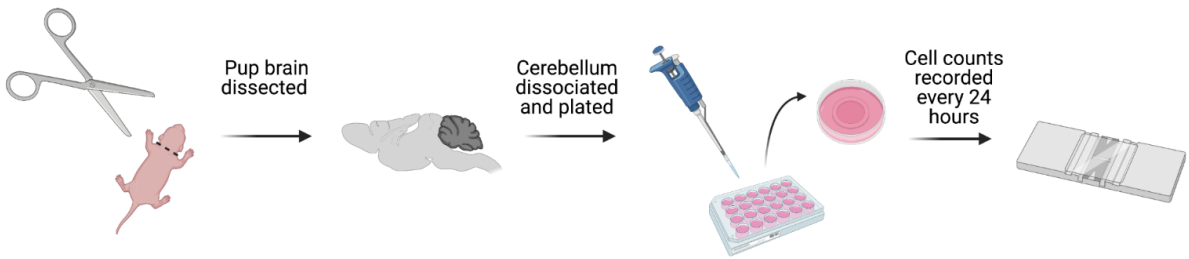

Fig. 4 | Workflow to collect cGNP cultures for proliferation experiments The brain is first dissected from a P7 mouse immediately after decapitation. After, the cerebellum is separated from the rest of the brain and dissociated using the Papain Dissociation, the cells are plated and treated with neurotransmitters for up to 72hrs before the cell counts are taken. Created with BioRender.

5. Evaluation of P7 cGNP Proliferation using EdU Incorporation

The Click-It® EdU Imaging Kit with Alexa Fluor® 594 Azide (Invitrogen, Cat. No. C10086) was used for this experiment. Additionally, a coverslip was added to each well of the 24-well plate in order to remove the adhered, incubated cultures for immunofluorescent staining. As with previous proliferation experiments, the cerebellar cultures harvested and dissociated from P7 mice were plated at $2x10^6$ cells /ml on Poly-D Lysine treated 24-well plates. Each well had 1uM SAG added to it and separate wells (with two technical replicates each) were segregated for the following treatments: 1mM L-glutamate, 50 uM GABA. Two wells per time point were treated with SAG alone as a positive control for proliferation. To label the cells with EdU, a 20uM EdU solution was prewarmed in complete medium and enough was added to each well to obtain a 10uM EdU solution. EdU incubation lasted for 6hrs and was followed by coverslip fixation in 500 uL of 4% PFA. The coverslip was incubated for 10 minutes before the PFA was aspirated and 500 uL of PBS was pipetted. The plate would then be stored at 4C. Next, the 1x Click-It buffer additive and Click-It reaction cocktail was prepared per the Click-It EdU Imaging Kit's instructions. The PBS was aspirated from the coverslips which were twice washed in 500uL of PBS. The EdU detection and DNA staining protocols for Alexa594 detection was followed per the The Click-It® EdU Imaging Kit instructions. The slides were then stored at 4C until they were imaged using a Zeiss LSM880 Laser Scanning Confocal Microscope at the RI-MUHC Molecular Imaging Platform with an excitation at 594 nm to detect EdU amongst the DAPI stained nuclei. Manual cell counts were then performed on each image to determine the number of EdU+ and EdU- cells. At least 500 cells were counted in two bilogical replicates (>10HPF per technical replicate).

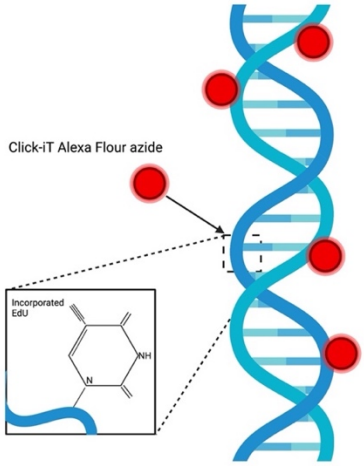

Fig. 5 | EdU Click-It Incorporation Diagram 5-ethynyl-2'-deoxyuridine (EdU) is a thymidine analogue that replaces thymidine bases in de-novo synthesized DNA templates. It applies a "click" chemistry reaction, using Click-It Alexa Flour azide, to detect the new thymidine analogue in cells. The reaction is a copper-catalyzed [3+3] cycloaddition where a stable triazole ring is formed by covalently coupling the alkyne group present in EdU to Alexa Fluor-conjugated azide group. Created with BioRender.

6. Assessment of glutamate production in post-natal cerebellum cultures

To assess glutamate production during cerebellum development, the cerebella of C57BL6 mice were dissected at key developmental time points (P5, P10, P15, P21) using the Sigma Aldrich Glutamate Assay Kit (SKU MAK330-1KT). The cGNP dissociation was performed on the cerebella as described in Method 2. Cell suspension was obtained from dissociated cerebella and the centration was diluted to $4x10^6$ cells/ml. These cells were then plated on a 24-well plate at 250µl per well, so each well contained $1x10^6$ cells. The amount of glutamate in the supernatant was determined after a 4hrs incubation using the Glutamate Assay Kit. The glutamate-dependent reaction is monitored by appearance of a coloured product, so the amount of glutamate in the cell media can be determined by measuring the absorbance of the reaction product at 450nm. (Fig. 6) As per the Glutamate Assay Kit protocol, 25 uL of the

supernatant collected from the incubated cerebella cultures was added to the reaction mix. All colorimetric measurements were done using the Tecan Infinite 200 Pro plate reader. A standard curve was generated by assaying a series of wells with standard amounts of glutamate added to and plotting the glutamate amount versus the absorbance of the resulting reaction product at 450nm. The glutamate content of each experimental sample was determined using the equation of the standard curve graph, inputting the measured absorbance of the sample at 450nm as the dependent variable and solving for the amount of glutamate in each sample. The following equation of the line was used to calculate the nmol of glutamate from each technical replicate.

$$y = 0.0644x + 0.238$$

To calculate the concentration of glutamate that was originally in 250µl of supernatant collected from the incubated cGNP cultures, the following dilution calculation was conducted. The technical replicates were averaged for each biological replicate and the means for all biological replicate (3-4 independent cGNPs preparations per time point) were visualised as a Tukey box plot.

$$mM\ glutamate = \frac{(nmol\ glutamate)}{(reaction\ volume\ ul)} * dilution\ factor$$

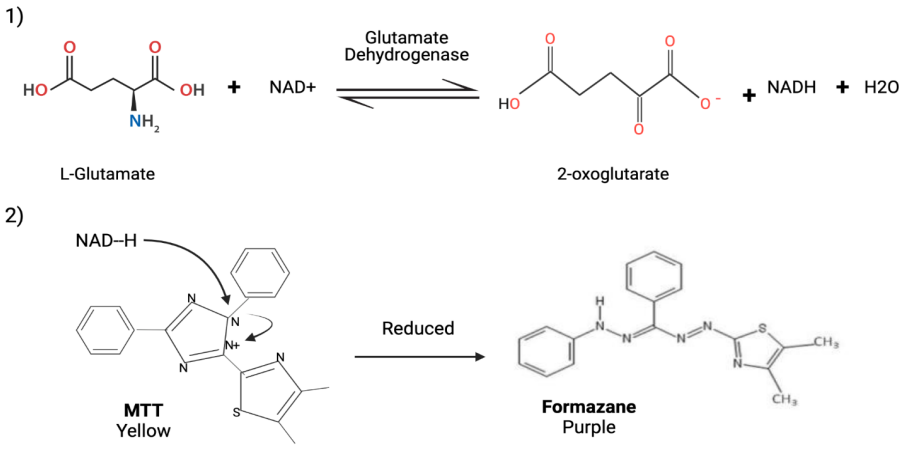

Fig. 6 | Reaction mechanism for the colorimetric glutamate assay The oxidation of glutamate is catalyzed by glutamate dehydrogenase. NADH then reduces MTT to create formazane, a colorimetric product. The intensity

of product colour measured at 450 nm is proportionate to the glutamate concentration in solution. Created with BioRender.

7. Measuring spontaneous neural activity in the developing mouse cerebellum using RNA in-situ hybridization

Using Method 1 C57BL6 mice were decapitated at several developmental time points (P7, P14, P21). Their brains were placed in OCT blocks and kept frozen at -80°C. The brains were sliced into 15µm sagittal sections and mounted onto slides and, once it was time to conduct the experiment, the slides were immersed in 4% PFA chilled at 4 degrees for 15 min. After being rinsed in 1x PBS wash buffer twice, the slides were placed in the following sequencing of EtOH dilutions for 5 min each at room temperature: 50% EtOH, 70% EtOH, 100% EtOH, 100% EtOH. After the last soak, the slides were air dried at room temperature for 5 mins. A hydrophobic barrier pen was then used to draw a barrier around the brain tissue and allowed to dry once more for 5 min. Next, 5 drops of protease IV from the RNAscope Fluorescent Multiplex Detection Reagents from ACD Bio (#320851) were added to the sample on the slide. The slide was incubated at room temperature for 30 minutes. Meanwhile, the HybEZ oven was heated to 40 degrees and the probes were warmed in a 40-degree water bath for 10 min and cooled to room temperature. Once the 30 min incubation was over, the excess protease was flicked off each slide and then dipped in 1x PBS 3-5 times for a wash. The slides were then transferred to the Humidity Control Tray for the HybEZ oven and 5 drops of c-fos and math1 were added to the slides. The tray was then placed into the HybeEZ oven for 2 hours at 40 degrees. After the incubation time was over, the slide holder was placed in a wash tray with 1X PBS and rocked for 2 minutes. This was process was repeated a second time and the same wash method was repeated between each incubation here after. After the excess liquid was shaken from the slides, 4 drops of Amp1-Fl were added to each sample. The slides were then reinserted into the HbyEZ Oven for 30 min and then the 1X PBS wash was used. The same

process was repeated for the Amp 2-Fl (15 min incubation), Amp3-Fl (30 min incubation), and Amp4-Fl (15 min incubation). One important note is that the Amp 4-Fl has 3 different fluorescent labels (A, B, and C). For c-fos and math1, the ideal label was Amp 4-Fl C. After the last 1X PBS wash was complete, the excess liquid was removed from the slides and ~4 drops of DAPI from the kit were added to each section. This was then covered with tin foil and incubated for 30 seconds at RT. Excess DAPI was removed from the slides and immediately after 1-2 drops of ProLong Gold Antifade Mountant were added to each slide. Coverslips were then placed on top of the samples and the slides were placed in a case to store in the dark at 4C.

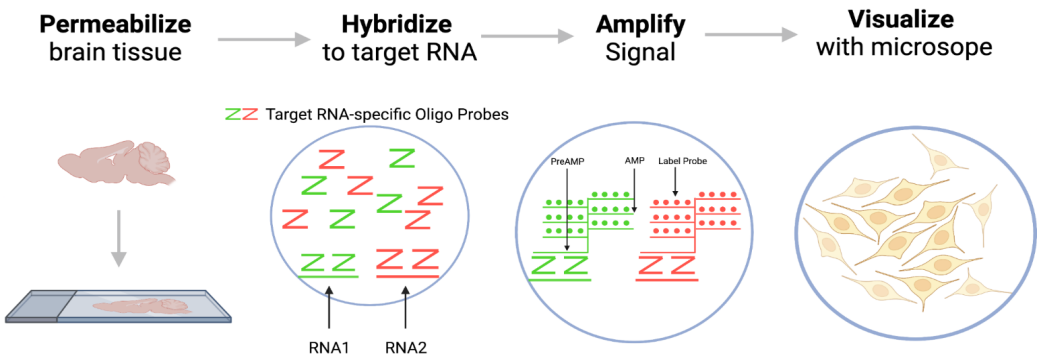

Fig. 7 | Schematic for the ACD Biotech RNAscope protocol Up to four probes, as well as DAPI staining of the nuclei, can be detected simultaneously. The separate probe channels available are C1, C2, C3, and C4 visible with their respective FITC, Cy3, Cy5, and Texas Red dyes. After the tissue is permeabilized to the slide, the lower portion of the double Z probe hybridizes to the specific RNA target. The upper portion of the probe is assigned to a specific probe channel after which the probes can be detected via microscopy. Created with BioRender.

8. Quantifying c-fos expression using ImageJ

Imaging was conducted on the Zeiss LSM880 Laser Scanning Confocal Microscope at the RI-MUHC Molecular Imaging Platform. The tiff files were separated by RBG channels in ImageJ to quantify and qualify the expression of c-fos, math1, and DAPI fluorescence. A mask was

placed on the sections of the EGL, ML, and IGL of the cerebellum in order to distinguish where expression of c-fos and math-1 were occurring. Using the freehand tool in ImageJ, each layer was selected for and the integrated density (IntDen) of c-fos fluorescence was recorded. The same process was applied for the int- and ext-EGL. In order to obtain to correlate the amount of fluorescence accruing in each layer of the developing cerebellum per the number of cells each one contained, the IntDen of DAPI was also measured. The final measurement was obtained by dividing the background corrected c-fos fluorescence (IntDen) by the IntDen of DAPI and the results were visualized in a Tukey Plot using GraphPad Prism software.

Chapter 3: Results

1. Depolarizing Neurotransmitters Exhibit an Anti-Proliferative Effect on Cerebellum Cultures

We compared the proliferation of CGNPs in culture treated with a Shh Agonist (SAG), L-glutamate, and GABA. Glutamate and GABA are both prominent neurotransmitters in the cerebellum, and in P7 mice, GABA is still an excitatory neurotransmitter (Young & Bordey, 2009). Therefore, we hypothesized that GABA and glutamate would have similar effects on CGNP expansion *in vitro*.

In Fig. 8, we observed that even in the presence of SAG, there is a statically significant decrease in proliferation for the cells treated with GABA and L-glutamate after the first 24 hours. This phenomenon continued over the 72-hr time period whereas cells treated with SAG alone remained proliferative. The effects of in vitro CGNP cultures, from excised mouse cerebellum, treated with neurotransmitters suggest that both GABA and L-glutamate exhibit an anti-proliferative effect on cGNPs and may be causing the cells to become unresponsive to SAG. If the result is due to depolarising events, then the similarity between the outcomes of the GABA and L-glutamate treated wells are to be expected as they are both depolarising NT. Further experimentation are planned to repeat the proliferation

trials again with glutamate antagonists, CNQX, D-AP5 and inhibitors of metabotropic glutamate receptors in order to narrow down which receptors might be involved in this phenomenon.

To compound the results in Fig. 8, an EdU (5-ethynyl-2′-deoxyuridine) assay was conducted on P7 cGNP cultures. The treated wells were composed of SAG and L-glutamate + SAG in order to observe if the addition of the depolarising neurotransmitter would decrease the amount of actively replicating cells, despite the presence of SAG. After conducting cell counts of EdU+ cells, it was observed that there was a significant decrease in actively proliferating cells in the L-glutamate wells compared to cells treated with SAG alone. (Fig. 9)

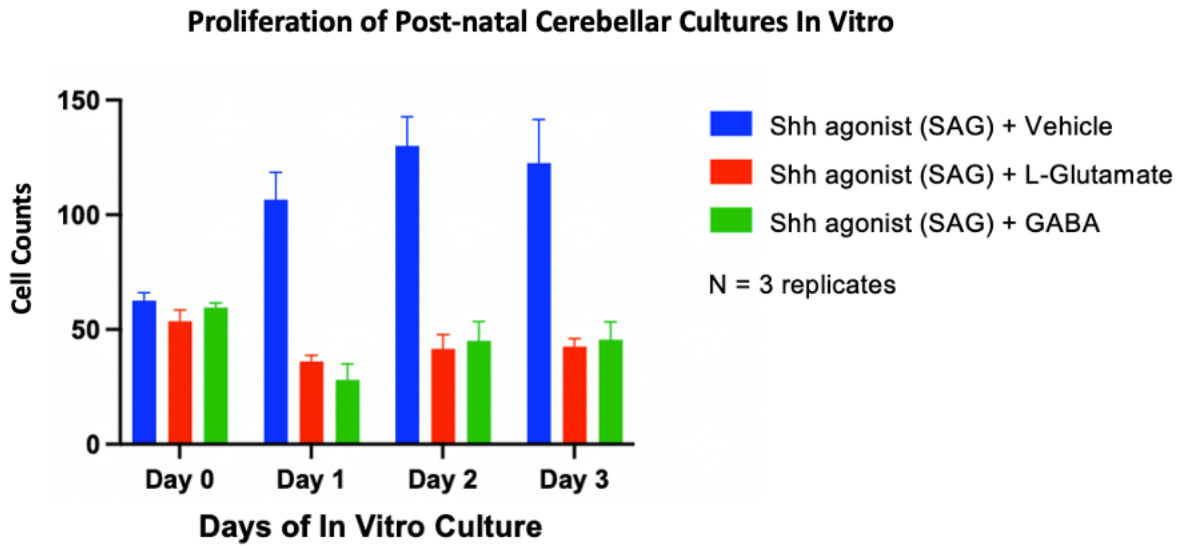

Fig. 8 | P7 cGNP proliferation in response to depolarising neurotransmitters P7 cerebellum were collected and dissociated for plating over a 72-hour time period to observe the effects of L-glutamate, GABA, and SAG on proliferation. Once cerebellum cultures were plated and dissociated via the Papain Dissociation System, SAG, L-glutamate (1mM), and GABA (50uM) were added to their respective treatment wells. Cell counts were taken every 24hrs using a haematocytometer and SAG was added to the cultures for an overnight treatment. Three independent experiments were performed. Cell counts were normalized. The addition of L-glutamate and GABA to the cultures had a statistically significant anti-proliferative effect, even in the present of SAG. A Mann-Whitney t-test was conducted to compare the experimental values to the vehicle control. Both L-glutamate and GABA had the same p-value ($p = 0.0286 < 0.05$) when compared to the vehicle.

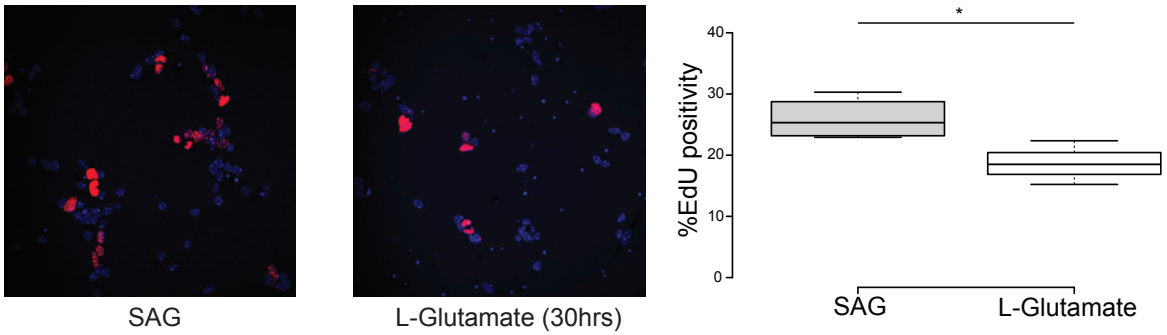

Fig. 9 | Quantification of EdU expression in P7 cGNP cultures P7 cerebellum were harvested and dissociated using the Papain Dissociation System. Cells were plated at $2x10^6$ cells / ml and SAG as well as L-glutamate were immediately added to the plate. Blue represents DAPI at 450nm and the red fluorescence is EdU at 598 nm. Two biological replicates were performed and imaging was conducted on a confocal microscope at 63x. Counts were taken manually and the percentage of Edu+ cells in the control (SAG) compared to the treated (L-glutamate) were plotted as a boxplot in R. There was a significant decrease observed between the EdU signaling in L-glutamate treated cells versus SAG alone by the 30 hr mark (p=0.042).

2. Glutamate is Produced During Early Stages of Cerebellum Development

To test our hypothesis that the CGNPs were being exposed to glutamate early in development and pre-disposing mutations may be affecting their ability to respond to the presence of glutamate in Shh MB I conducted a colorimetric glutamate assay. One condition of this model is that throughout development, glutamate must be produced in the cerebellum. This assay helps to answer this question with the objective of demonstrating and quantifying the amount of glutamate in the developing mouse cerebellum cultures excised at p5, p10, p15, and p21. The glutamate measured in this experiment was solely from in vitro granule cell cultures which does not necessarily translate to what might be occurring in vivo. Results in Fig. 10 display that glutamate is even present early in development (P5) as well as around peak proliferation (P7). The concentration of glutamate produced by cerebella cultures

experiences a statistically significant increase with age. Welsch's t-test was applied in R to compare the concentrations of secreted glutamate between developmental time points.

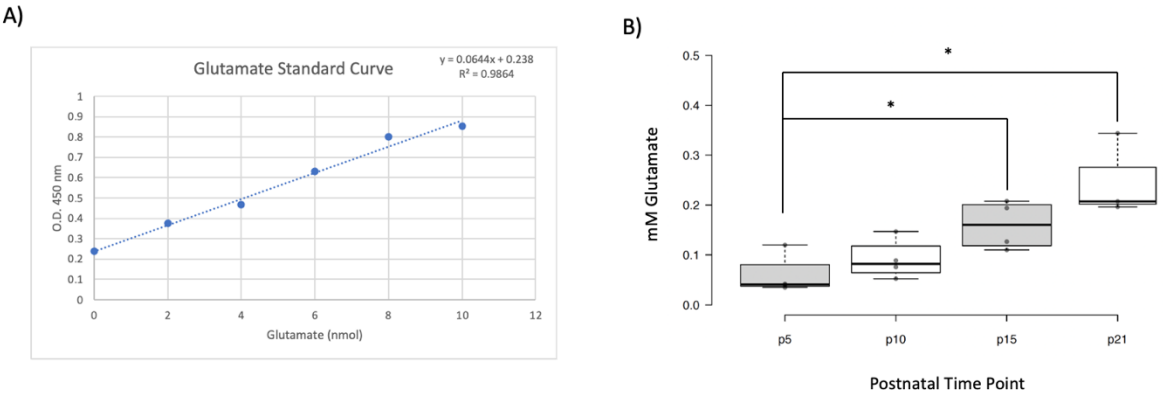

Fig. 10 | Production of glutamate during post-natal cerebellum development A) A standard curve was created with known concentrations of glutamate in order to derive the equation of the line to calculate the nmol of glutamate from experimental colorimetric readings. B) Colorimetric assay of murine cerebella glutamate production at 5, 10, 15, and 21 days post-natal. The cerebella were collected at each time point and dissociated using the Papain Dissociation System. The assay determining the amount of glutamate produced was conducted using the Sigma Aldrich Glutamate Assay Kit. Colorimetric measurements were read at 450nm. Four biological replicates were performed. Glutamate is shown to be present early in development at comparable amounts at P5 and P10 and increases significantly by P15 ($p = 0.01913964 < 0.05$) and P21 ($p = 0.00942004 < 0.05$). Center lines show the medians; box limits indicate the 25th and 75th percentiles as determined by R software; whiskers extend 1.5 times the interquartile range from the 25th and 75th percentiles, outliers are represented by dots. n = 4, 4, 4, 3 sample points.

3. Spontaneous Neural Activity is an Early Event in Cerebellum Development

As the presence of glutamate is not equivalent to neural circuit activity, it is important to demonstrate that with the increase in glutamate during murine brain development, there is also an increase in neural activity. For Aim 3, I used an RNA In-situ hybridization study to detect the spontaneous neuronal activity in the cerebellum that could be caused by glutamate. Cell depolarisation results in the immediate transcription of the immediate-early gene c-fos which will act as my proxy for the neuronal activity. In Fig. 11 (A-B), I detected the expression of c-fos within the EGL of the cerebellum at P7 and P14 before synaptic connections are even

formed. In Fig. 11C, the expression of c-fos is solely allocated to the IGL as the EGL disappears by P21.

The second probe used for a co-expression study with c-fos was Math1. (Fig 13) Math1 is a transcription factor expressed only by cGNPs in the EGL and it is required for cGNP genesis. In Fig. 12, we observed c-fos signal, indication of probable spontaneous neural activity, localised to both the external EGL (overlapping with Math1 expression) and the int-EGL (outside math1 expressing region) where there is cell cycle arrest and cell migration begins. Quantification of c-fos expression within the different layers of cerebellum cytoarchitecture revealed a statistically significant difference in expression between the EGL and ML as well as the EGL and the IGL. (Fig. 13A) When the quantified expression of c-fos was compared between the ext- and int-EGL, there was no significant difference between the data sets. (Fig. 13B)

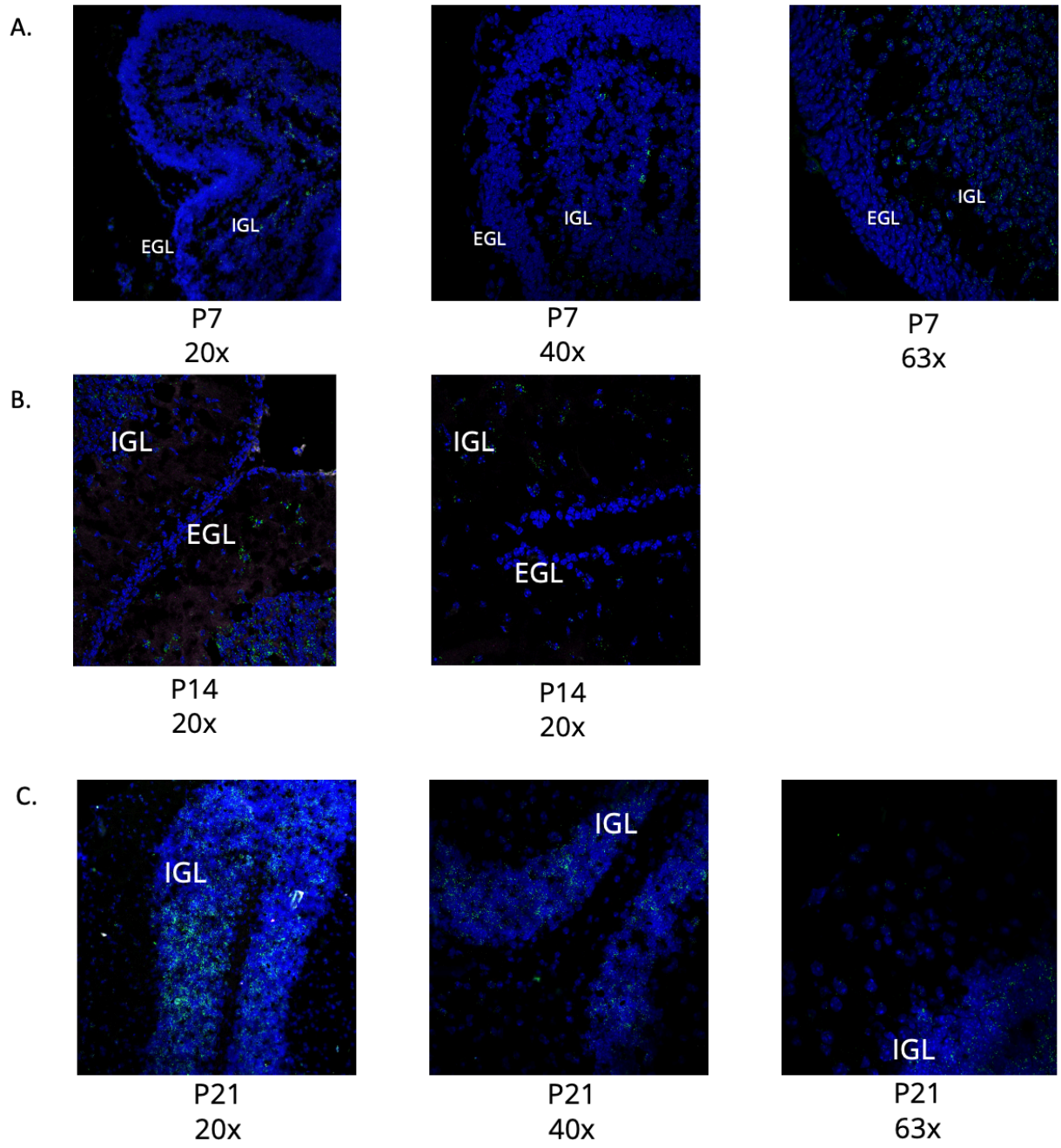

Fig. 11 | Expression of c-fos in mouse cerebella during post-natal development Images of sliced, murine brains using ACD Confocal Microscope to image c-fos RNA in-situ hybridization. Green fluorescence indicates c-fos, the signal for spontaneous neural activity and proxy for the presence of glutamate. 7A represents p7, 7B represents p14, and 7C represents p21. C-fos is present in early development at P7 and P14 within the EGL and IGL of the cerebellum indicating neuronal activity is occurring before mature neurons and synaptic events are formed. By P21 the presence of c-fos is allocated to the IGL as the EGL has dissipated.

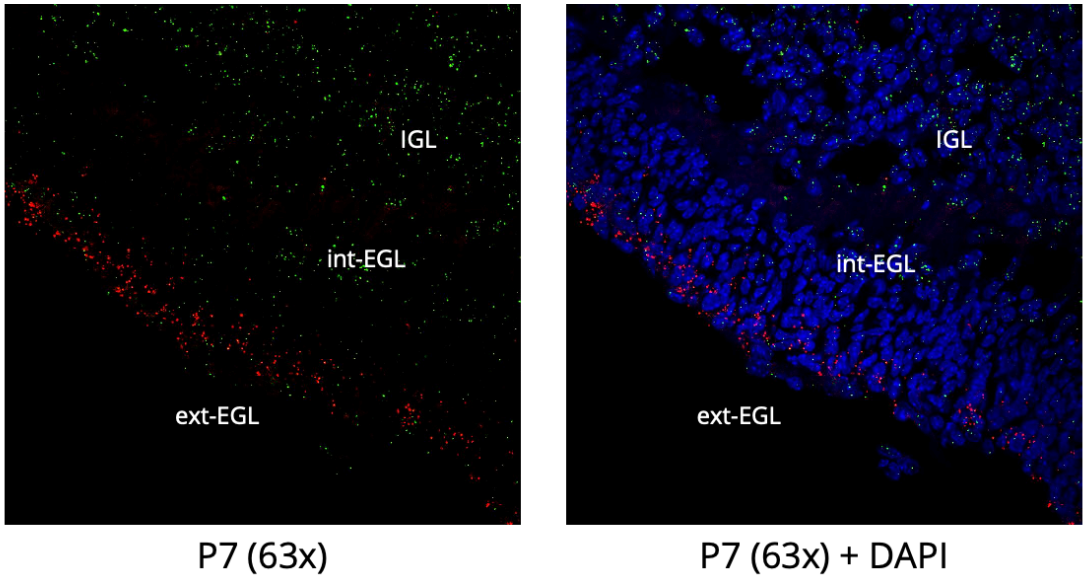

Fig. 12 | Co-expression of math1 and c-fos in P7 mouse cerebella Images of sliced, P7 murine brains using ACD Confocal Microscope to image the co-expression of c-fos and math1 RNA in-situ hybridization. Math1 expression is observed in the ext-EGL, where it is highly concentrated, as well as in the int-EGL where it overlaps with c-fos expression. C-fos positive signal is observed where proliferating, undifferentiated cGNPs are located and not only in the IGL where synaptic events are formed by mature neurons.

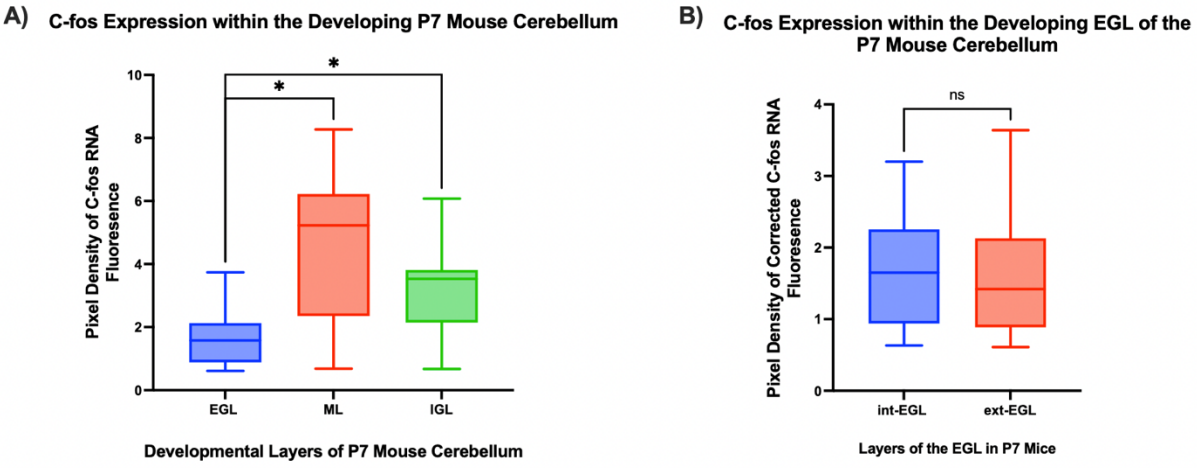

Fig. 13 | Quantification of c-fos expression in P7 mouse cerebellum A) A Tukey plot was used to display the quantification of pixel density of c-fos RNA fluorescence within the cytoarchitecture of a P7 cerebellum. This graph displays the 25% and 75% with the extreme bars and there are no outliers because they would be represented as individual dots on the graph above the bars. The middle line represents the median. Between the EGL and ML ($p = 0.0188 < 0.05$) and the EGL and IGL ($p = 0.04 < 0.05$) there was a significant difference in expression of c-fos. There is no significant difference between the ML and the IGL ($p = 0.03401$). B) The same Tukey plot was applied to the

quantified pixel density of c-fos RNA fluorescence within the int- and ext-EGL of the same P7 cerebella. There is no significant difference ($p = 0.8819$) in c-fos expression between the two layers of the EGL.

Chapter 4: Discussion

With the lab's pre-established premise of cell depolarisation initiating MB tumour cells tumour suppressive effect, our lab aimed to establish a model that demonstrated the importance of glutamate counterbalancing the proliferative effects of the Shh pathway during cerebellum development. Unpublished research from the lab produced prior to this thesis demonstrated that electrical activity is tumour suppressive in Shh MB. Publications outside of the Garzia lab have also established the important role of neural activity during the development of the central nervous system and, more specifically, its control of cell population expansion and differentiation in neural precursor cells (Spitzer, 2006). Building upon this work, the first aim of this thesis was to establish the *in vitro* effects of glutamate and GABA on the proliferation of cGNPs harvested from P7 mice (when cGNPs reach peak proliferation in post-natal mice) (Manto & Huisman, 2018; Roussel & Hatten, 2011). To begin, the dissociated cGNPs were treated with SAG in order to simulate the stimulation of Shh mitogenic signal during early post-natal expansion in the cerebellum (Lewis et al., 2004). In Fig. 8, the cells treated with SAG alone experience an increase in cell counts over the 72-hr time period. This is expected as Shh signalling is the major driver of cGNP proliferation within the cerebellum; an increase in cultured populations should be observed in SAG treated cells compare(Nguyen et al., 2018). Other studies have even demonstrated that the addition of SAG to cGNP cultures will not only promote proliferation but rescue cGNPs from cerebellar hypoplasia and downregulated Shh signalling (Nguyen et al., 2018). The cells in culture should also be highly proliferative and responsive to SAG as they were obtained from P7 mice which is when peak proliferation in the developing cerebellum occurs. Individual wells were also treated with either L-glutamate (its active form) or GABA. The former neurotransmitter was selected as it's the major neurotransmitter in the brain. The second NT, GABA, was also selected as many cerebellar cell types (such as Purkinje neurons, basket

cells, and stellate12 cells) are GABAergic and granule neurons express GABA receptors (Dave & Bordey, 2009). Despite being the main inhibitory neurotransmitter in the mature central nervous system, GABA also exhibits depolarising effects in the immature brain (Dave & Bordey, 2009). The presence of GABA receptors lends to the possibility that GABA's own depolarising events could be initiating cGNPs' post-mitotic state and migration in vivo to induce the transient influx of Ca2+ (an important secondary messenger for neurons) in cGNPs (Dave & Bordey, 2009). In Fig. 8, we observed that despite the presence of SAG, the cGNPs experience a significant decrease in proliferation for the cells treated with L-glutamate and GABA after the first 24hrs. This phenomenon continued over the following 72hr time period whereas the cells treated with SAG alone remained proliferative. The only significant difference between data sets was found when comparing the vehicle to GABA and glutamate, separately; there was no significant difference between the experimental treatments. If the result is solely due to a depolarising event, then the similarity between the outcomes of GABA and L-glutamate treated cGNPs are to be expected as they are both depolarising neurotransmitters. These results compound Dr. Garzia's unpublished work, suggesting that GABA and L-glutamate exhibit an anti-proliferative effect on cGNPs; their presence inducing depolarising events in cGNPs which cause the cells to become post-mitotic and begin their migration towards the IGL to differentiate into mature neurons and become unresponsive to the Shh mitogen on their journey. Because GABA demonstrates a similar decrease in CGNP proliferation to glutamate during early brain development, this supports the idea that depolarising, not a precise metabolic effect of glutamate, is driving the anti-proliferative effects on cGNPs.

As cells counts are not the most definitive method to determine active, or inactive, cell division, we conducted further experimentation using 5-ethynyl-2'-deoxyuridine (EdU) (a

thymidine analogue and marker for newly synthesized DNA). EdU is considered as the gold-standard to assess cell proliferation as it allows us to quantify the percentage of cGNPs synthesizing DNA by fluorescent detection via click chemistry. The incorporation of EdU into the de novo-synthesized DNA replaces thymidine base pairs and becomes permanently labeled into the proliferating cells and subsequent daughter cells. The Alexa Fluor-conjugated azide group used for this experiment is small allowing it to easily diffuse into the cells to access the EdU nucleosides in the tagged DNA; the detection of the fluorescent EdU marker would act as the indicator for active cell duplication occurring in vitro. This assay is also sensitive in nature as it does not subject the cells to a harsh round of treatments (trypsin, HCL, heat, and/or DNase) like BrdU incorporation protocol (Mead & Lefebvre, 2014). One potential room for error, however, is that thymidine analogs can generate mutations and DNA damage in some instances (thereby affecting the cell cycle) and the EdU label can become diluted over multiple rounds of cell division (Mead & Lefebvre, 2014).

Upon quantification of the EdU cell counts, there was a statistically significant decrease in active cell division between the SAG treated cells and those treated with L-glutamate as well as SAG after 30 hours of treatment. The decrease in proliferation of cGNPs when treated with L-glutamate, despite the presence of a Shh agonist, further solidifies our hypothesis that depolarising events generated in the presence of glutamate are inducing cell cycle arrest of cGNPs during development. Future attempts at successfully replicating the SAG and neurotransmitter treatments of EdU tagged cGNP cultures not only to confirm the results found in Fig.9 but to narrow down the responsible receptor for glutamate-induced depolarising events in cGNPGs. These would include the addition of receptor antagonist D-AP5 (an NMDA receptor antagonist that completes with glutamate binding) and CNQX (an AMPA/kainate receptor antagonist). Furthermore, it will be necessary to perform longer

treatment of cGNP cultures with selected drugs or NTs followed by EdU pulsing and staining to see if the decrease of EdU incorporation rate decreases further. Since I observed a higher effect of NTs on cell counts than it would be warranted by the decrease observed in EdU incorporation rate, it is possible that toxicity effects are also present, on the post-mitotic IGL granule neurons, and influencing the results in Fig. 8. The excitotoxity of glutamate has been previously demonstrated in cerebellum granule neurons derived from chicken embryos or rat pups although this is usually correlated with synaptic maturation which occurs after DIV3 in culture (Yadav et al., 2021).

For GABAergic cortical interneurons born in the caudal ganglionic eminence, electrical activity is crucial for their ability to migrate (De Marco García, Karayannis, & Fishell, 2011). Further in development, glutamate-mediated activity is necessary for these neurons to develop their axons and dendrites (De Marco García et al., 2011). When exposed to kainate, or GABA, neural precursor cells of the ventricular zone (VZ) in rat models had their proliferation reduced (LoTurco et al., 1995). Meanwhile, if they were exposed to the antagonists for AMPA, kainate, or GABA receptors their rates of cell division would increase (LoTurco et al., 1995). What LoTurco et al. discovered was that the anti-proliferative effects observed in the rats were dependent on the function of voltage-gated calcium channels (VGCCs) which aligns with our lab hypothesis of neural activity being the halting factor for proliferation (LoTurco et al., 1995). In the immature rat hippocampi, granule neuron precursors differentiate in response to depolarization, and this response is also dependent on VGCCs (Boyden, Zhang, Bamberg, Nagel, & Deisseroth, 2005). In ex vivo MB patient samples, the expression of the metabotropic glutamate receptor mGluR4 was also found to be correlated with an increased 5-year survival inversely corresponding to recurrence and metastasis (Iacovelli et al., 2006). When human MB cell lines were treated with the mGluR4

receptor agonist PHCC it led to a decrease in proliferation as well as reduced growth of the xenografted MB cell lines in mice (Iacovelli et al., 2006). PHCC injections also prevented the development of MB in Ptch heterozygous mice (Iacovelli et al., 2006). However, it is important to note that depolarization is not always pro-differentiation nor anti-proliferation; these effects seem to be dependent not only on the cell type but also the time point in development the neural activity is introduced. One such example is how hippocampal granule neuron precursors differentiate in response to electrical activity (Imoto et al., 2017). However, granule cells isolated from the adult mouse hippocampus undergo a 'dematuration' when exposed to the same stimuli and express markers (and electrophysiology) usually related to their immature counterparts (Imoto et al., 2017). When D-AP5 is introduced to block NMDA receptors, the effect of electrical stimulation to these cells is attenuated (Imoto et al., 2017). Depending on the results of future proliferation assays including CNQX and AP-5, it would be interesting to investigate the necessity of factors such as VGCCs, NMDARs, CREB, and certain protein kinases in the anti-proliferative effects of depolarization on CGNPs. In current literature, it is unclear how the effects of depolarisation range vastly between different cell types and time points in development and further emphasizes the need to successfully replicate the EdU cGNP experiments with the addition of glutamate and GABA receptor antagonists.

Understanding glutamate's effects with cGNPs during early cerebellum development can only be relevant to the hypothesis of this thesis if glutamate is present during key post-natal stages. I proceeded to conduct a colorimetric glutamate assay to investigate twofold: mature cGNPs directly secrete more glutamate their immature counterparts and to observe whether cGNPs are exposed to glutamate in early development. If so, we can further hypothesize that pre-disposing mutations in cGNPs may be affecting their ability to respond to the presence of

glutamate to halt proliferation at key developmental timepoints in mice (such as P7). This assay helps to answer this question with the objective of demonstrating and quantifying the amount of glutamate in CGNP cultures at P5, P10, P15, and P21. Since the chemical reaction of glutamate with glutamate dehydrogenase is specific to the L-isomer (and unreactive to other glutamic acid derivatives such as glutamine, D-glutamate, and L-aspartate), the specificity of the reaction is very high. However, inaccurate timing of NAD solution to the blank and sample can lead to false values either in the standard curve or colorimetric reading of the sample so precise timing is necessary.

In Fig. 10B, supernatant collected from the supernatant of P21 (maturity) and P15 (early post-migratory) cGNP cultures had a statistically higher production of glutamate compared to the cultures harvested from P5 (early post-natal) mice. This supports the notion that as the number of differentiated cGNPs increases in the IGL at later developmental time points, their production of glutamate equally grows. Our hypothesis extends further proposing that the glutamate being produced diffuses towards the undifferentiated cGNPs of the EGL to cause anti-prolific neural activity. From this, we can also expect to see an increase in neural activity within the cerebellar cytoarchitecture of P15 and p21 mice compared to younger pups. This is to be expected as cGNP proliferation in mice is completed within the two postnatal weeks; by P15, the cerebellum has already produced the necessary amount of differentiated cGNPs that will, hypothetically, be secreting glutamate (Rahimi-Balaei et al., 2018). The presence of glutamate in vitro at P10 and P5 demonstrates as well that glutamate is present in early cerebellum development (even during the cerebellum's most proliferative state, P7) yet does not exactly reflect what may be occurring in vivo. As early exposure to glutamate and its depolarising effects might be crucial for cerebellum development, we can also hypothesize that MB predisposing mutations may be affecting cGNP's ability to respond to glutamate as

early as P5. As these are cerebellum cultures and not isolated cGNP cultures, we cannot guarantee that the only cells producing glutamate within this experiment are cGNPs alone. However, cGNPs are the most numerous neurons in the cerebellum and most other neurons are GABAergic allotting for the statement that the glutamate harvested from the supernatant is primarily produced by the cGNPs in culture (Hoshino et al., 2005; Wechsler-Reya & Scott, 1999)

Aside from determining the presence of glutamate in cerebellar cultures at different time points during post-natal development, the colorimetric assay also serves a secondary purpose. In order to develop novel therapeutic targets that may simulate anti-tumorigenic depolarising events in Shh MB patients, it is important to elucidate the correct target receptors associated with our proposed model. By determining the concentration of glutamate at key points of cGNP proliferation and differentiation, the glutamate receptors that may be involved with anti-prolific cell depolarisation events may be determined by their EC50 (effective concentration 50%); what concentration of glutamate is necessary to obtain 50% of its bioactivity whether it is for inhibition or activation (Maréchal, 2011). EC50 values allow for the comparison of different molecules effects on a biological component and are generally used to measure bioactivity occurring in vivo but can also be applied for in vitro analysis of partial enzyme inhibitors. The main drawback, however, is that EC50 is unable to provide any information on the efficacy of the activated / inhibited receptor. Unpublished research from the Garzia lab revealed, through a subgroup-specific expression analysis of glutamate receptors, a tumour-specific downregulation of both ionotropic and metabotropic glutamate receptor genes in in both human and mouse Shh MB samples. The findings focused on the anti-tumorigenic properties of metabotropic glutamate receptors *Grm1* and *Grm5* agonists (CHPG and DHPG, respectfully) both in vitro and in vivo. Using concentrations from the

colorimetric assay, the ionotropic receptors associated with both glutamate and Shh MB can be postulated. Accordingly, different pathways can lead to the transcriptional activation or suppression of ionotropic or metabotropic receptor genes. By studying how glutamate receptor expression is regulated, we may be able to better understand the underlying mechanisms they're silenced in Shh MB tumours and find potential targets for cancer immunotherapy in order to reverse this downregulation.

Current literature indicates that, in cerebellar granule cells, the EC50 of L-glutamate required to activate AMPA receptors is hundreds of umoles/L (depending on subtypes) whereas NMDA receptors are in the low uM range (Damschroder-Williams, Irwin, Lin, & Paul, 1995; Morimoto-Tomita et al., 2009). From the results in Fig. 10B, we can observe that at P10, the median amount of glutamate in vitro (0.08 mM) is sufficient to activate NMDA receptors during early cerebellum development. Blocking NMDA receptors with D-AP5 and MK-801 agonists has already been proven to successfully decrease the rates of granule cell migration in the ML whereas using treating cGNPs in vitro with CNQX to block AMPA glutamate receptors had no effect (Komuro et al., 2021). The importance of NMDA activation in glutamate-induced cGNP migration is further supported as alterations to Mg2+, which obstructs NMDA activity in a voltage-dependent manner, decreases granule cell migration as well, especially in the ML (Komuro et al., 2021). Furthermore, previous research has provided evidence that cGNP NMDA receptor sensitivity towards glutamate, within the EGL, increases as post-natal cerebellum development progresses which correlates to increased migration in later stages (Komuro et al., 2021). This supports the theory of our model that extracellular endogenous glutamate in the EGL, diffusing from differentiated cells in the IGL, induces depolarising events via NMDA receptors to promote cell migration during early hindbrain development. Since the granule cells are immature, the glutamate signaling would

be evoked in a paracrine manner and the phenomena of nonsynaptic activation of NMDA via glutamate has already been observed in migrating cGNPs (Komuro et al., 2021). As our EdU experiments are honed, we can cross reference the results from the receptor agonist effects on proliferation with the glutamate concentration at that time point in mouse cerebellum development. Further experimentation to observe whether NMDA receptor activation may be occurring as early as P7, when cGNPs are their most proliferative, should be considered as well.

In vitro detection of glutamate and cell depolarisation's anti-proliferative effects are not sufficient to support our hypothesis that neural activity impairs oncogenic transformation of cGNPs, nor can we correlate that the production of glutamate in the immature cerebellum means it is the origin of said neural activity. As the presence of glutamate is not equivalent to neural circuit activity, it is important to demonstrate that with the increase in glutamate during murine brain development, there is also an increase in neural activity. To provide further evidence, the next goal of this thesis was to localize and quantify cell depolarisation events within the in vivo cytoarchitecture of post-natal mouse cerebella. To conduct these experiments, a dual probe RNA in situ hybridization was performed on OCT-slices of P7, P14, and P21 mouse brains. C-fos was selected as my probe to evaluate spontaneous neural activity and to also act as my proxy for glutamate as when glutamate produces a depolarising event, the immediate transcript of the early gene c-fos occurs within the first 5 minutes of electrical stimulation. The limitation, however, is that the presence of c-fos does not directly correlate to glutamate as other depolarising neurotransmitters (such as GABA) can also cause depolarising events to occur during early development. We expected to observe more c-fos expression in later stages of development (P14 and P21) since the mice will have development more coordinated neurons by then to walk which means more differentiated

cells in the IGL. The second probe we selected was math1/atoh1 because it is a transcription factor expressed in cGNPs of the EGL as math1 is required for cGNP genesis. Since the EGL disappears by P21, so should math1 expression. An overexpression of math1 has also been observed in Shh MB tumours as well which is postulated to be associated with the overproduction of cGNP proliferation occurring in Shh MB tumour tissue. The kit selected for this experiment was the ACD Biotech RNAscope due to its heightened specificity and simultaneous detection of multiple RNA targets. This was ideal for the co-expression of math1 and c-fos. The key advantage of the double-Z probe provided by this kit is the significant signal boost it provides which simultaneously suppresses background noise.

In Fig. 12 (A-B), I detected the expression of c-fos within the EGL of the cerebellum at P7 and P14 before synaptic connections are even formed. Since the cells begin to express the c-fos marker before they form synapses, this indicates that they could be exposed to neurotransmitters in the EGL before arriving in the IGL. In Fig 13C, the expression of c-fos is solely allocated to the IGL as the EGL disappears by P21. In Fig. 12, where the co-expression of c-fos and math1 was detected in P7 mouse cerebella, we observed a significant increase in spontaneous neural activity localised to the int-EGL (overlapping with Math1 expression) where there is cell cycle arrest and cell migration and differentiation begin. These results indicate that the expression and manifestation of neural activity is an early event in differentiation in granule cells. The math1/c-fos results indicate that the expression and manifestation of neural activity is an early event in differentiation in granule cells yet more expression studies at different time points throughout development should be conducted in the future. To compound the visual results of math1 / c-fos co-expression, the intensity of c-fos expression was also measured between the EGL, ML, and IGL using ImageJ (Fig. 13A). When quantifying these measurements, the area of the cerebellum layer was taken into

account in order to normalize the data. Interestingly, spontaneous neural activity was observed in all three layers of the P7 cerebellum which in the EGL and ML means that spontaneous neural activity is occurring where the synapses of mature neurons are not present. Where c-fos overlaps with math1 expression also confirms that these events are taking place within the EGL. This evidence supports the model that glutamate diffuses from the IGL towards the EGL and the cell depolarising events it causes along the way are counterbalancing a parallel Shh gradient and lead to spontaneous neural activity in the EGL which induces cGNP migration. In Fig. 13A, it can also be observed that the ML contains the highest expression of c-fos The same process was also conducted to compare expression between the int- and ext-EGL (Fig. 13B). However, there was no significant different of c-fos expression between the int- and ext- EGL that might suggest depolarising events are localised to a specific section of the EGL.

To cleanly and specifically test the role of membrane depolarization in the pathogenesis of medulloblastoma, we pursued an optogenetic approach, since many drugs and small molecules targeting neurotransmitter pathways have off-target effects. HChR2 is a rapidly gated, blue light-sensitive cation channel suitable for non-invasive control of membrane potential. It can be activated by illumination with blue light (470nm), inducing a flux of positive ions through the membrane resulting in membrane depolarization (Boyden et al., 2005). Unpublished in vivo results in the Garzia lab have also demonstrated that optogenetically-driven membrane depolarization could attenuate the malignant phenotype, engraftment, and survival of transgenic Ptch/hChR2 medulloblastoma mice. Currently, we are analysing the RNA sequencing data from mouse Ptch/hChR2 Shh MB cells that were optogenetically photostimulated in vitro to assess the effects of depolarization on gene expression. RNA sequencing results were analysed to retrieve a list of differentially

expressed genes (DEGs) in the light stimulated group. From this list, DEGs associated with neurotransmitter activity, cellular modified amino acid metabolic processes, and the regulation of cell population proliferation were selected for further analysis. I have designed primers to confirm these results via RT-PCR. Of special interest, *GRM1* (metabotropic glutamate receptor) and *GRIA1* (heteromeric glutamate receptor) were upregulated in the light stimulated group. This couples with the unpublished results previously discovered in the lab demonstrating the downregulated of both genes in human and mouse Shh MB tumour cells. Elucidating the pathways affected by the light-induced depolarization in cGNPs could help uncover the mechanisms behind the effects that depolarization is having on the proliferation and differentiation and uncover new targets in the effort to treat MB. In future experiments, our lab plans to use a lentiviral vector containing humanized channelrhodopsin-2 (hChR2) to infect human Shh and Group 4 MB cells. The cells will be treated with blue light to induce depolarization and then their proliferation will be assessed using methods such as BrdU16 incorporation, Ki67 staining, cell counts, and cell cycle analysis. The photostimulated cells will be injected intracranially into immunocompromised mice to determine whether depolarisation influences their ability to form tumours and affect mouse survival.

How glutamate and neural activity can have such diverse effects on different cell types and cancers remains unclear. Out of the current literature, a common theme in neuronal proliferation and differentiation is the dependence of Ca2+ entry into the cells (either by NMDA or VGCCs). This is not surprising considering that Ca2+ is a very important second messenger, has the able to alter gene expression and synaptic plasticity in neurons, and mediates potentials that precedes synapse formation crucial to neural development (Berridge, 1998; Kawamoto, Vivar, & Camandola, 2012; Schüller et al., 2008; Spitzer, 2006). More so,

the radial migration of cGNPs from the EGL towards the IGL is regulated by the amplitude and frequency in fluctuations of Ca2+ (Komuro et al., 2021). Ca2+-dependent synaptic plasticity mechanisms might also be similar to the mechanisms involved with depolarisation of cGNP through glutamate that lead to cell migration and differentiation in cerebellum development. Ca2+-dependent synaptic plasticity mechanisms might also be similar to the mechanisms involved with depolarisation of cGNP through glutamate that lead to cell migration and differentiation in cerebellum development. Yang et al. observed that as intracellular concentrations of Ca2+ increase, the potentiation or depression of synapses can occur depending on which cell type is being stimulated (Colbran, 2004; Shen, Zhou, & Yang, 1999). Similar to how Ca2+ induces a series of phosphorylation events in the adult cerebellum to incite synaptic plasticity which leads to the phosphorylation of CREB (targeting NeuroD, an essential regulator of cGNP differentiation) the Shh mitogen causes the dephosphorylation of CREB (Sheng & Kim, 2002). Thus, depolarising events that might be induced in proliferating cGNPs by the presence of glutamate (or GABA) may be directing the phosphorylation of CREB and counterbalancing the effects of Shh signalling.

In conclusion, the current experiments have provided support for the Garzia lab's model that neural activity impair oncogenic transformation of cerebral granule neuron precursors and is tumour suppressive in Shh MB (Fig. 14). The rationale was that a glutamate gradient is secreted by differentiated neurons of the IGL which diffuses dorsally towards the EGL through the ML and counterbalances a parallel Shh mitogenic signal. However, While the anti-proliferative effects of L-glutamate and GABA on cGNPs were demonstrated in vitro, further experimentation (such addition of receptor antagonists) to support the model is required. Overall, the mechanisms of neural activity remain an interesting avenue to investigate novel, non-toxic treatments for Shh MB patients.

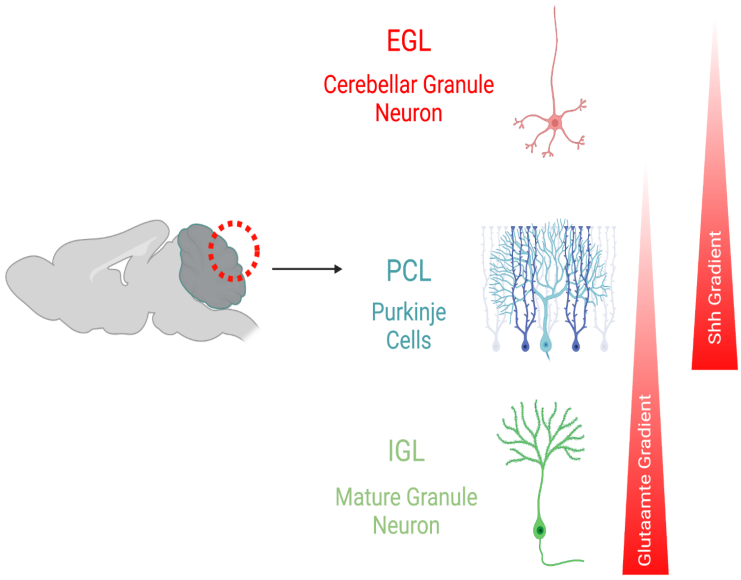

Fig. 14 | Proposed model for post-natal cerebellum development A glutamate gradient originating from the differentiated cells of the IGL diffuses towards the undifferentiated cells of the EGL. Once the proliferating cells of the int-EGL are exposed to glutamate, cell depolarization is initiated leading to the migration and differentiation of cGNPs against the Shh gradient towards the IGL; the post-mitotic cells no longer responsive to the Shh mitogen. Created with BioRender.

References

Ahn, S., & Joyner, A. L. (2005). In vivo analysis of quiescent adult neural stem cells responding to Sonic hedgehog. *Nature, 437*(7060), 894-897.

Anderson, P. R., Hanlon, A. L., Patchefsky, A., Al-Saleem, T., & Hanks, G. E. (1998). Perineural invasion and Gleason 7-10 tumors predict increased failure in prostate cancer patients with pretreatment PSA< 10 ng/ml treated with conformal external beam radiation therapy. *International Journal of Radiation Oncology* Biology* Physics, 41*(5), 1087-1092.

Ayrault, O., Zhao, H., Zindy, F., Qu, C., Sherr, C. J., & Roussel, M. F. (2010). Atoh1 inhibits neuronal differentiation and collaborates with Gli1 to generate medulloblastoma-initiating cells. *Cancer research, 70*(13), 5618-5627.

Ayrault, O., Zindy, F., Rehg, J., Sherr, C. J., & Roussel, M. F. (2009). Two tumor suppressors, p27Kip1 and patched-1, collaborate to prevent medulloblastoma. *Molecular Cancer Research, 7*(1), 33-40.

Azevedo, F. A., Carvalho, L. R., Grinberg, L. T., Farfel, J. M., Ferretti, R. E., Leite, R. E., . . . Herculano-Houzel, S. (2009). Equal numbers of neuronal and nonneuronal cells make the human brain an isometrically scaled-up primate brain. *Journal of Comparative Neurology, 513*(5), 532-541.

Barrera, M., Shaw, A. K., Speechley, K. N., Maunsell, E., & Pogany, L. (2005). Educational and social late effects of childhood cancer and related clinical, personal, and familial characteristics. *Cancer, 104*(8), 1751-1760.

Barthelery, N. J., & Manfredi, J. J. (2016). Cerebellum development and tumorigenesis: a p53-centric perspective. *Trends in molecular medicine, 22*(5), 404-413.

Bartkowska, K., Paquin, A., Gauthier, A. S., Kaplan, D. R., & Miller, F. D. (2007). Trk signaling regulates neural precursor cell proliferation and differentiation during cortical development.

Batsakis, J. (1985). Nerves and neurotropic carcinomas. *The Annals of otology, rhinology, and laryngology, 94*(4 Pt 1), 426-427.

Berridge, M. J. (1998). Neuronal calcium signaling. *Neuron, 21*(1), 13-26.

Borghesani, P. R., Peyrin, J. M., Klein, R., Rubin, J., Carter, A. R., Schwartz, P. M., . . . Segal, R. A. (2002). BDNF stimulates migration of cerebellar granule cells.

Boyden, E. S., Zhang, F., Bamberg, E., Nagel, G., & Deisseroth, K. (2005). Millisecond-timescale, genetically targeted optical control of neural activity. *Nature neuroscience, 8*(9), 1263-1268.

Buckner, R. L. (2013). The cerebellum and cognitive function: 25 years of insight from anatomy and neuroimaging. *Neuron, 80*(3), 807-815.

Butts, T., Green, M. J., & Wingate, R. J. (2014). Development of the cerebellum: simple steps to make a 'little brain'. *Development, 141*(21), 4031-4041.

Canettieri, G., Di Marcotullio, L., Greco, A., Coni, S., Antonucci, L., Infante, P., . . . Miele, E. (2010). Histone deacetylase and Cullin3–REN KCTD11 ubiquitin ligase interplay regulates Hedgehog signalling through Gli acetylation. *Nature cell biology, 12*(2), 132-142.

Canudas, A., Di Giorgi-Gerevini, V., Iacovelli, L., Nano, G., D'onofrio, M., Arcella, A., . . . Battaglia, G. (2004). PHCCC, a specific enhancer of type 4 metabotropic glutamate receptors, reduces proliferation and promotes differentiation of cerebellar granule cell neuroprecursors. *Journal of Neuroscience, 24*(46), 10343-10352.

Carballo, G. B., Honorato, J. R., & de Lopes, G. P. F. (2018). A highlight on Sonic hedgehog pathway. *Cell Communication and Signaling, 16*(1), 1-15.

Cavalli, F. M., Remke, M., Rampasek, L., Peacock, J., Shih, D. J., Luu, B., . . . Morrissy, A. S. (2017). Intertumoral heterogeneity within medulloblastoma subgroups. *Cancer cell, 31*(6), 737-754. e736.

Chakroborty, D., Chowdhury, U. R., Sarkar, C., Baral, R., Dasgupta, P. S., & Basu, S. (2008). Dopamine regulates endothelial progenitor cell mobilization from mouse bone marrow in tumor vascularization. *The Journal of clinical investigation, 118*(4), 1380-1389.

Chizhikov, V. V., Lindgren, A. G., Mishima, Y., Roberts, R. W., Aldinger, K. A., Miesegaes, G. R., . . . Millen, K. J. (2010). Lmx1a regulates fates and location of cells originating from the cerebellar rhombic lip and telencephalic cortical hem. *Proceedings of the National Academy of Sciences, 107*(23), 10725-10730.

Cohen Jr, M. M. (2003). The hedgehog signaling network. *American journal of medical genetics Part A, 123*(1), 5-28.

Colbran, R. J. (2004). Protein phosphatases and calcium/calmodulin-dependent protein kinase II-dependent synaptic plasticity. *Journal of Neuroscience, 24*(39), 8404-8409.

Damschroder-Williams, P., Irwin, R. P., Lin, S. Z., & Paul, S. M. (1995). Characterization of the excitoprotective actions of N-Methyl-D-Aspartate in cultured cerebellar granule neurons. *Journal of neurochemistry, 65*(3), 1069-1076.

Dave, K. A., & Bordey, A. (2009). GABA increases Ca2+ in cerebellar granule cell precursors via depolarization: implications for proliferation. *IUBMB life, 61*(5), 496-503.

De Marco García, N. V., Karayannis, T., & Fishell, G. (2011). Neuronal activity is required for the development of specific cortical interneuron subtypes. *Nature, 472*(7343), 351-355.

Englund, C., Kowalczyk, T., Daza, R. A., Dagan, A., Lau, C., Rose, M. F., & Hevner, R. F. (2006). Unipolar brush cells of the cerebellum are produced in the rhombic lip and migrate through developing white matter. *Journal of Neuroscience, 26*(36), 9184-9195.

Finlay, J. L., Erdreich-Epstein, A., & Packer, R. J. (2007). Progress in the treatment of childhood brain tumors: no room for complacency. *Pediatric hematology and oncology, 24*(1), 79-84.

Flora, A., Klisch, T. J., Schuster, G., & Zoghbi, H. Y. (2009). Deletion of Atoh1 disrupts Sonic Hedgehog signaling in the developing cerebellum and prevents medulloblastoma. *science, 326*(5958), 1424-1427.

Fogarty, M. P., Emmenegger, B. A., Grasfeder, L. L., Oliver, T. G., & Wechsler-Reya, R. J. (2007). Fibroblast growth factor blocks Sonic hedgehog signaling in neuronal precursors and tumor cells. *Proceedings of the National Academy of Sciences, 104*(8), 2973-2978.

Fujita, S. (1967). Quantitative analysis of cell proliferation and differentiation in the cortex of the postnatal mouse cerebellum. *The Journal of Cell Biology, 32*(2), 277-287.

Fults, D. W., Taylor, M. D., & Garzia, L. (2019). Leptomeningeal dissemination: a sinister pattern of medulloblastoma growth. *Journal of Neurosurgery: Pediatrics, 23*(5), 613-621.

Furukawa, H., Singh, S. K., Mancusso, R., & Gouaux, E. (2005). Subunit arrangement and function in NMDA receptors. *Nature, 438*(7065), 185-192.

Gajjar, A., Chintagumpala, M., Ashley, D., Kellie, S., Kun, L. E., Merchant, T. E., . . . Krasin, M. J. (2006). Risk-adapted craniospinal radiotherapy followed by high-dose chemotherapy and stem-cell rescue in children with newly diagnosed

medulloblastoma (St Jude Medulloblastoma-96): long-term results from a prospective, multicentre trial. *The lancet oncology, 7*(10), 813-820.

Gajjar, A. J., & Robinson, G. W. (2014). Medulloblastoma—translating discoveries from the bench to the bedside. *Nature reviews Clinical oncology, 11*(12), 714-722.

Green, M. J., & Wingate, R. J. (2014). Developmental origins of diversity in cerebellar output nuclei. *Neural development, 9*(1), 1-8.

Haldipur, P., Dang, D., Aldinger, K. A., Janson, O. K., Guimiot, F., Adle-Biasette, H., . . . Millen, K. J. (2017). Phenotypic outcomes in Mouse and Human Foxc1 dependent Dandy-Walker cerebellar malformation suggest shared mechanisms. *Elife, 6*, e20898.

Harada, H., Sato, T., & Nakamura, H. (2016). Fgf8 signaling for development of the midbrain and hindbrain. *Development, growth & differentiation, 58*(5), 437-445.

Helms, A. W., Abney, A. L., Ben-Arie, N., Zoghbi, H. Y., & Johnson, J. E. (2000). Autoregulation and multiple enhancers control Math1 expression in the developing nervous system. *Development, 127*(6), 1185-1196.

Hinoi, E., Fujimori, S., Takarada, T., Taniura, H., & Yoneda, Y. (2002). Facilitation of glutamate release by ionotropic glutamate receptors in osteoblasts. *Biochemical and biophysical research communications, 297*(3), 452-458.

Holgado, B. L., Guerreiro Stucklin, A., Garzia, L., Daniels, C., & Taylor, M. D. (2017). Tailoring medulloblastoma treatment through genomics: making a change, one subgroup at a time. *Annual review of genomics and human genetics, 18*, 143-166.

Hollmann, M., & Heinemann, S. (1994). Cloned glutamate receptors. *Annual review of neuroscience, 17*(1), 31-108.

Hong, E. J., McCord, A. E., & Greenberg, M. E. (2008). A biological function for the neuronal activity-dependent component of Bdnf transcription in the development of cortical inhibition. *Neuron, 60*(4), 610-624.

Hoshino, M., Nakamura, S., Mori, K., Kawauchi, T., Terao, M., Nishimura, Y. V., . . . Sone, M. (2005). Ptf1a, a bHLH transcriptional gene, defines GABAergic neuronal fates in cerebellum. *Neuron, 47*(2), 201-213.

Iacovelli, L., Arcella, A., Battaglia, G., Pazzaglia, S., Aronica, E., Spinsanti, P., . . . Gulino, A. (2006). Pharmacological activation of mGlu4 metabotropic glutamate receptors inhibits the growth of medulloblastomas. *Journal of Neuroscience, 26*(32), 8388-8397.

Jimsheleishvili, S., & Dididze, M. (2020). Neuroanatomy, cerebellum. *StatPearls [Internet]*.

Kalariti, N., Lembessis, P., & Koutsilieris, M. (2004). Characterization of the glutametergic system in MG-63 osteoblast-like osteosarcoma cells. *Anticancer research, 24*(6), 3923-3930.

Kawamoto, E. M., Vivar, C., & Camandola, S. (2012). Physiology and pathology of calcium signaling in the brain. *Frontiers in pharmacology, 3*, 61.

Kenney, A. M., Cole, M. D., & Rowitch, D. H. (2003). Nmyc upregulation by sonic hedgehog signaling promotes proliferation in developing cerebellar granule neuron precursors.

Kenney, A. M., & Rowitch, D. H. (2000). Sonic hedgehog promotes G1 cyclin expression and sustained cell cycle progression in mammalian neuronal precursors. *Molecular and cellular biology, 20*(23), 9055-9067.

Klisch, T. J., Xi, Y., Flora, A., Wang, L., Li, W., & Zoghbi, H. Y. (2011). In vivo Atoh1 targetome reveals how a proneural transcription factor regulates cerebellar development. *Proceedings of the National Academy of Sciences, 108*(8), 3288-3293.

Komiya, Y., & Habas, R. (2008). Wnt signal transduction pathways. *Organogenesis, 4*(2), 68-75.

Komuro, Y., Kumada, T., Ohno, N., Fahrion, J. K., Foote, K. D., Fenner, K. B., . . . Komuro, H. (2021). Granule cell migration and differentiation. In *Handbook of the Cerebellum and Cerebellar Disorders* (pp. 139-171): Springer.

Kool, M., Korshunov, A., Remke, M., Jones, D. T., Schlanstein, M., Northcott, P. A., . . . Van Vuurden, D. (2012). Molecular subgroups of medulloblastoma: an international meta-analysis of transcriptome, genetic aberrations, and clinical data of WNT, SHH, Group 3, and Group 4 medulloblastomas. *Acta neuropathologica, 123*(4), 473-484.

Kuzan-Fischer, C. M., Juraschka, K., & Taylor, M. D. (2018). Medulloblastoma in the molecular era. *Journal of Korean neurosurgical society, 61*(3), 292.

Labrakakis, C., Patt, S., Hartmann, J., & Kettenmann, H. (1998). Functional GABAA receptors on human glioma cells. *European Journal of Neuroscience, 10*(1), 231-238.

Lawn, S., Krishna, N., Pisklakova, A., Qu, X., Fenstermacher, D. A., Fournier, M., . . . Kenchappa, R. S. (2015). Neurotrophin signaling via TrkB and TrkC receptors promotes the growth of brain tumor-initiating cells. *Journal of Biological Chemistry, 290*(6), 3814-3824.

Leto, K., Bartolini, A., Yanagawa, Y., Obata, K., Magrassi, L., Schilling, K., & Rossi, F. (2009). Laminar fate and phenotype specification of cerebellar GABAergic interneurons. *Journal of Neuroscience, 29*(21), 7079-7091.

Leto, K., Carletti, B., Williams, I. M., Magrassi, L., & Rossi, F. (2006). Different types of cerebellar GABAergic interneurons originate from a common pool of multipotent progenitor cells. *Journal of Neuroscience, 26*(45), 11682-11694.

Levisohn, L., Cronin-Golomb, A., & Schmahmann, J. D. (2000). Neuropsychological consequences of cerebellar tumour resection in children: cerebellar cognitive affective syndrome in a paediatric population. *Brain, 123*(5), 1041-1050.

Lewis, P. M., Gritli-Linde, A., Smeyne, R., Kottmann, A., & McMahon, A. P. (2004). Sonic hedgehog signaling is required for expansion of granule neuron precursors and patterning of the mouse cerebellum. *Developmental biology, 270*(2), 393-410.

Lin, T.-H., Yang, R.-S., Tang, C.-H., Wu, M.-Y., & Fu, W.-M. (2008). Regulation of the maturation of osteoblasts and osteoclastogenesis by glutamate. *European journal of pharmacology, 589*(1-3), 37-44.

Liu, Y., Elf, S. E., Miyata, Y., Sashida, G., Liu, Y., Huang, G., . . . Menendez, S. (2009). p53 regulates hematopoietic stem cell quiescence. *Cell stem cell, 4*(1), 37-48.

LoTurco, J. J., Owens, D. F., Heath, M. J., Davis, M. B., & Kriegstein, A. R. (1995). GABA and glutamate depolarize cortical progenitor cells and inhibit DNA synthesis. *Neuron, 15*(6), 1287-1298.

Louis, D. N., Perry, A., Reifenberger, G., Von Deimling, A., Figarella-Branger, D., Cavenee, W. K., . . . Ellison, D. W. (2016). The 2016 World Health Organization classification of tumors of the central nervous system: a summary. *Acta neuropathologica, 131*(6), 803-820.

Luzzi, S., Lucifero, A. G., Brambilla, I., Mantelli, S. S., Mosconi, M., Foiadelli, T., & Savasta, S. (2020). Targeting the medulloblastoma: A molecular-based approach. *Acta Bio Medica: Atenei Parmensis, 91*(Suppl 7), 79.

Manto, M., & Huisman, T. A. (2018). *The Cerebellum: From Embryology to Diagnostic Investigations: Handbook of Clinical Neurology Series*: Elsevier.

Maréchal, E. (2011). Measuring Bioactivity: KI, IC50 and EC50. In (pp. 55-65): Springer Berlin Heidelberg.

Mead, T. J., & Lefebvre, V. (2014). Proliferation assays (BrdU and EdU) on skeletal tissue sections. In *Skeletal Development and Repair* (pp. 233-243): Springer.

Millen, K. J., Steshina, E. Y., Iskusnykh, I. Y., & Chizhikov, V. V. (2014). Transformation of the cerebellum into more ventral brainstem fates causes cerebellar agenesis in the absence of Ptf1a function. *Proceedings of the National Academy of Sciences, 111*(17), E1777-E1786. doi:10.1073/pnas.1315024111

Morales, D., & Hatten, M. E. (2006). Molecular markers of neuronal progenitors in the embryonic cerebellar anlage. *Journal of Neuroscience, 26*(47), 12226-12236.

Morimoto-Tomita, M., Zhang, W., Straub, C., Cho, C.-H., Kim, K. S., Howe, J. R., & Tomita, S. (2009). Autoinactivation of Neuronal AMPA Receptors via Glutamate-Regulated TARP Interaction. *Neuron, 61*(1), 101-112. doi:10.1016/j.neuron.2008.11.009

Moxon-Emre, I., Bouffet, E., Taylor, M. D., Laperriere, N., Scantlebury, N., Law, N., . . . Mabbott, D. (2014). Impact of craniospinal dose, boost volume, and neurologic complications on intellectual outcome in patients with medulloblastoma. *Journal of Clinical Oncology, 32*(17), 1760-1768.

Nguyen, V., Sabeur, K., Maltepe, E., Ameri, K., Bayraktar, O., & Rowitch, D. H. (2018). Sonic hedgehog agonist protects against complex neonatal cerebellar injury. *The Cerebellum, 17*(2), 213-227.

Northcott, P. A., Jones, D. T., Kool, M., Robinson, G. W., Gilbertson, R. J., Cho, Y.-J., . . . Taylor, M. D. (2012). Medulloblastomics: the end of the beginning. *Nature Reviews Cancer, 12*(12), 818-834.

Parant, J., Chavez-Reyes, A., Little, N. A., Yan, W., Reinke, V., Jochemsen, A. G., & Lozano, G. (2001). Rescue of embryonic lethality in Mdm4-null mice by loss of Trp53 suggests a nonoverlapping pathway with MDM2 to regulate p53. *Nature genetics, 29*(1), 92-95.

Pastorino, L., Ghiorzo, P., Nasti, S., Battistuzzi, L., Cusano, R., Marzocchi, C., . . . Scarrà, G. B. (2009). Identification of a SUFU germline mutation in a family with Gorlin syndrome. *American journal of medical genetics Part A, 149*(7), 1539-1543.

Pazzaglia, S., Tanori, M., Mancuso, M., Gessi, M., Pasquali, E., Leonardi, S., . . . Covelli, V. (2006). Two-hit model for progression of medulloblastoma preneoplasia in Patched heterozygous mice. *Oncogene, 25*(40), 5575-5580.

Peterson, S. C., Eberl, M., Vagnozzi, A. N., Belkadi, A., Veniaminova, N. A., Verhaegen, M. E., . . . Wong, S. Y. (2015). Basal cell carcinoma preferentially arises from stem cells within hair follicle and mechanosensory niches. *Cell stem cell, 16*(4), 400-412.

Pietsch, T., Schmidt, R., Remke, M., Korshunov, A., Hovestadt, V., Jones, D. T., . . . Kool, M. (2014). Prognostic significance of clinical, histopathological, and molecular characteristics of medulloblastomas in the prospective HIT2000 multicenter clinical trial cohort. *Acta neuropathologica, 128*(1), 137-149.

Platt, S. R. (2007). The role of glutamate in central nervous system health and disease–a review. *The Veterinary Journal, 173*(2), 278-286.

Pogoriler, J., Millen, K., Utset, M., & Du, W. (2006). Loss of cyclin D1 impairs cerebellar development and suppresses medulloblastoma formation.

Pomeroy, S. L., Tamayo, P., Gaasenbeek, M., Sturla, L. M., Angelo, M., McLaughlin, M. E., . . . Lau, C. (2002). Prediction of central nervous system embryonal tumour outcome based on gene expression. *Nature, 415*(6870), 436-442.

Rahimi-Balaei, M., Bergen, H., Kong, J., & Marzban, H. (2018). Neuronal migration during development of the cerebellum. *Frontiers in cellular neuroscience, 12*, 484.

Ramaswamy, V., Remke, M., Bouffet, E., Bailey, S., Clifford, S. C., Doz, F., . . . Milde, T. (2016). Risk stratification of childhood medulloblastoma in the molecular era: the current consensus. *Acta neuropathologica, 131*(6), 821-831.

Rose, M. F., Ahmad, K. A., Thaller, C., & Zoghbi, H. Y. (2009). Excitatory neurons of the proprioceptive, interoceptive, and arousal hindbrain networks share a developmental requirement for Math1. *Proceedings of the National Academy of Sciences, 106*(52), 22462-22467.

Roussel, M. F., & Hatten, M. E. (2011). Cerebellum: development and medulloblastoma. *Current topics in developmental biology, 94*, 235-282.

Schüller, U., Heine, V. M., Mao, J., Kho, A. T., Dillon, A. K., Han, Y.-G., . . . Qian, Y. (2008). Acquisition of granule neuron precursor identity is a critical determinant of progenitor cell competence to form Shh-induced medulloblastoma. *Cancer cell, 14*(2), 123-134.

Shen, Y., Zhou, Y., & Yang, X. L. (1999). Characterization of AMPA receptors on isolated amacrine-like cells in carp retina. *European Journal of Neuroscience, 11*(12), 4233-4240.

Sheng, M., & Kim, M. J. (2002). Postsynaptic signaling and plasticity mechanisms. *science, 298*(5594), 776-780.

Solecki, D. J., Liu, X., Tomoda, T., Fang, Y., & Hatten, M. E. (2001). Activated Notch2 signaling inhibits differentiation of cerebellar granule neuron precursors by maintaining proliferation. *Neuron, 31*(4), 557-568.

Spitzer, N. C. (2006). Electrical activity in early neuronal development. *Nature, 444*(7120), 707-712. doi:10.1038/nature05300

Sudarov, A., & Joyner, A. L. (2007). Cerebellum morphogenesis: the foliation pattern is orchestrated by multi-cellular anchoring centers. *Neural development, 2*(1), 1-22.

Sudarov, A., Turnbull, R. K., Kim, E. J., Lebel-Potter, M., Guillemot, F., & Joyner, A. L. (2011). Ascl1 genetics reveals insights into cerebellum local circuit assembly. *Journal of Neuroscience, 31*(30), 11055-11069.

Swanson, D. J., & Goldowitz, D. (2011). Experimental Sey mouse chimeras reveal the developmental deficiencies of Pax6-null granule cells in the postnatal cerebellum. *Developmental biology, 351*(1), 1-12.

Takano, T., Lin, J. H.-C., Arcuino, G., Gao, Q., Yang, J., & Nedergaard, M. (2001). Glutamate release promotes growth of malignant gliomas. *Nature medicine, 7*(9), 1010-1015.

Taylor, M. D., Northcott, P. A., Korshunov, A., Remke, M., Cho, Y.-J., Clifford, S. C., . . . Gajjar, A. (2012). Molecular subgroups of medulloblastoma: the current consensus. *Acta neuropathologica, 123*(4), 465-472.

Van Ommeren, R., Garzia, L., Holgado, B. L., Ramaswamy, V., & Taylor, M. D. (2020). The molecular biology of medulloblastoma metastasis. *Brain Pathology, 30*(3), 691-702.

Venkatesh, H., & Monje, M. (2017). Neuronal activity in ontogeny and oncology. *Trends in cancer, 3*(2), 89-112.

Venkatesh, H. S., Johung, T. B., Caretti, V., Noll, A., Tang, Y., Nagaraja, S., . . . Mitra, S. S. (2015). Neuronal activity promotes glioma growth through neuroligin-3 secretion. *Cell, 161*(4), 803-816.

Volpe, J. J. (2009). Cerebellum of the premature infant: rapidly developing, vulnerable, clinically important. *Journal of child neurology, 24*(9), 1085-1104.

Wang, S., Wei, X., Chen, B., Zhao, M., Song, G., Zhang, Z., & Li, N. (2016). Expression of metabotropic glutamate receptor 4 in osteosarcoma. *Molecular and clinical oncology, 4*(1), 65-69.

Wang, V. Y., Rose, M. F., & Zoghbi, H. Y. (2005). Math1 expression redefines the rhombic lip derivatives and reveals novel lineages within the brainstem and cerebellum. *Neuron, 48*(1), 31-43.

Wechsler-Reya, R. J., & Scott, M. P. (1999). Control of neuronal precursor proliferation in the cerebellum by Sonic Hedgehog. *Neuron, 22*(1), 103-114.

Wong, A. W., Xiao, J., Kemper, D., Kilpatrick, T. J., & Murray, S. S. (2013). Oligodendroglial expression of TrkB independently regulates myelination and progenitor cell proliferation. *Journal of Neuroscience, 33*(11), 4947-4957.

Wu, C., & Sun, D. (2015). GABA receptors in brain development, function, and injury. *Metabolic brain disease, 30*(2), 367-379.

Wu, G., Diaz, A. K., Paugh, B. S., Rankin, S. L., Ju, B., Li, Y., . . . Zhang, J. (2014). The genomic landscape of diffuse intrinsic pontine glioma and pediatric non-brainstem high-grade glioma. *Nature genetics, 46*(5), 444.

Yadav, A., Verhaegen, S., Verbruggen, E., Kerhoas, M., Huiberts, E. H. W., Hadera, M. G., . . . Paulsen, R. E. (2021). A human relevant mixture of persistent organic pollutants (POPs) and perfluorooctane sulfonic acid (PFOS) differentially affect glutamate induced excitotoxic responses in chicken cerebellum granule neurons (CGNs) in vitro. *Reproductive Toxicology, 100*, 109-119.

Yamada, M., Seto, Y., Taya, S., Owa, T., Inoue, Y. U., Inoue, T., . . . Hoshino, M. (2014). Specification of spatial identities of cerebellar neuron progenitors by ptf1a and atoh1 for proper production of GABAergic and glutamatergic neurons. *Journal of Neuroscience, 34*(14), 4786-4800.

Ye, Z.-C., & Sontheimer, H. (1999). Glioma cells release excitotoxic concentrations of glutamate. *Cancer research, 59*(17), 4383-4391.

Yeung, J., Ha, T. J., Swanson, D. J., & Goldowitz, D. (2016). A novel and multivalent role of Pax6 in cerebellar development. *Journal of Neuroscience, 36*(35), 9057-9069.

Young, S. Z., & Bordey, A. (2009). GABA's control of stem and cancer cell proliferation in adult neural and peripheral niches. *Physiology, 24*(3), 171-185.

Zanin, J. P., Abercrombie, E., & Friedman, W. J. (2016). Proneurotrophin-3 promotes cell cycle withdrawal of developing cerebellar granule cell progenitors via the p75 neurotrophin receptor. *Elife, 5*, e16654.

Zhao, H., Ayrault, O., Zindy, F., Kim, J.-H., & Roussel, M. F. (2008). Post-transcriptional down-regulation of Atoh1/Math1 by bone morphogenic proteins suppresses medulloblastoma development. *Genes & development, 22*(6), 722-727.

Zhao, Y., Chen, S., Swensen, A. C., Qian, W.-J., & Gouaux, E. (2019). Architecture and subunit arrangement of native AMPA receptors elucidated by cryo-EM. *science, 364*(6438), 355-362.